ACI Research Paper #10-2026

The Challenge of Regulating Dirty New Industries:

Evidence from Cryptocurrency Mining

Siddharth GEORGE

Zhihao HAN

Alberto SALVO

August 2026

Please cite this article as:

George, Siddharth, Zhihao Han and Alberto Salvo, "The Challenge of Regulating Dirty New Industries: Evidence from Cryptocurrency Mining", Research Paper #10-2026, *Asia Competitiveness Institute Research Paper Series (August 2026)*

The Challenge of Regulating Dirty New Industries: Evidence from Cryptocurrency Mining

Siddharth George[*], Zhihao Han[†], and Alberto Salvo[‡§]

July 23, 2026

Abstract

Computation-intensive digital industries are rapidly expanding, yet there is little evidence on how to decarbonise them. We examine two major efforts to decarbonise cryptocurrency mining. First, we evaluate China's cryptomining ban using a difference-in-differences design. The ban reduced electricity consumption and fossil-fuel generation in mining provinces, lowering China's total electricity use by 0.59%. In response, mining activity relocated: China exported more cryptomining equipment, which flowed to established US mining hubs. Electricity consumption increased in US mining states, powered by increased fossil generation, especially from old coal plants. This relocation attenuated the global impact of China's ban by one-third. Second, we examine Ethereum's transition to Proof-of-Stake, a cleaner production technology, using a regression discontinuity design. Ethereum's switch reduced US electricity consumption, but miners redeployed their equipment to mine substitute cryptocurrencies, diluting its impact. Our findings illustrate the difficulty of regulating emerging industries like AI that use mobile, multi-purpose production factors.

[*] Department of Economics, National University of Singapore, segeorge@nus.edu.sg

[†] Asia Competitiveness Institute, National University of Singapore, zhihao.hanaci@nus.edu.sg

[‡] Department of Economics, National University of Singapore, albertosalvo@nus.edu.sg

[§] We thank Lucas Davis, David Dorn, Xinming Du, Jonathan Elliot, Teevrat Garg, Chad Jones, Pete Klenow, David Lagakos, Martin Mattsson, Rohini Pande, Xiaoyue Shan, Joseph Shapiro, Ran Song, Tiffany Tsai, Olivier Deschenes, Xuezhen Tao, Ying Feng, Tong Liu, Yu Qin, Kamhon Kan, Wen-Chieh Lee, Zhiwei Xu, Qiaoyi Chen, Hendrik Wolff, and Dariusz Wojcik for useful discussions. We also thank seminar audiences at NUS, Columbia's graduate student conference, and the joint NUS-Government Economist Service workshop for helpful feedback.

1 Introduction

Economies are rapidly adopting computation-heavy technologies like artificial intelligence (AI). Yet these technologies consume vast amounts of energy at a time when societies must phase out carbon-intensive activities to combat climate change. Governments typically support the climate transition by regulating dirty industries (He et al., 2020) and promoting cleaner production technologies. However, absent comprehensive regulation such as a global carbon price, these efforts can be undermined if firms relocate dirty activities to jurisdictions with weaker regulation (Tanaka et al., 2022) or redeploy dirty production factors to unregulated uses. Such carbon leakage is especially difficult to prevent in digital industries, where production factors (e.g., data centres) are mobile, serve global markets, and have multiple uses. Despite the energy intensity and growing importance of these sectors, there is little empirical evidence on how to decarbonise them effectively.

We examine two major efforts to decarbonise the cryptocurrency industry—a growing sector that offers a useful laboratory to evaluate emissions reduction policies in computation-heavy industries more broadly. Cryptocurrencies rely on a production technology called a consensus mechanism to verify and process transactions.[1] In the most widely used consensus mechanism, Proof-of-Work (PoW), miners compete to solve mathematical puzzles; the winner gains the right to validate transactions and earn cryptocurrency rewards. To compete effectively, miners run large amounts of specialised computing hardware, making cryptomining highly energy-intensive. Engineering estimates suggest that mining Bitcoin—which comprises 51% of the cryptocurrency market—consumes as much electricity as the Netherlands, though estimates vary with modelling assumptions (Foteinis, 2018; De Vries et al., 2022).[2] Despite the industry's size and emissions intensity (Papp et al., 2023), evidence on how to reduce the energy use of cryptomining is scarce.

Leveraging subnational Chinese and US data on cryptomining activity, electricity use, and trade, we evaluate two policies that aimed to reduce the carbon intensity of cryptomining. Both policies reduced emissions in the markets they targeted, but each triggered a distinct form of leakage that diluted its global impact. First, we study China's cryptomining ban, and estimate its impact on domestic electricity consumption and generation.

[1]Most cryptocurrencies use blockchain technology to secure transactions and rely on a decentralised consensus mechanism for verifying transaction blocks and updating the blockchain (see section 2).

[2]The Cambridge Blockchain Sustainability Index uses a weighted average for mining equipment energy efficiency and daily hashrates to calculate the network electricity consumption rate. Other estimates (e.g., from the Crypto Carbon Ratings Institute) are based on the global distribution of selected mining hardware and the number of nodes in each country.

Then, we examine the ban's global spillovers: we show that mining activity relocated, weakening the ban's global impact. Second, we analyse the transition of Ethereum, the second-largest cryptocurrency, from PoW to a cleaner consensus mechanism. We estimate how Ethereum's transition affected energy consumption and document that miners diluted its impact by redeploying their machines to mine substitute cryptocurrencies.

Energy is a key input for computation-heavy digital activities such as cryptomining. Thus, cryptominers tend to locate in places with cheap and abundant electricity. Data compiled by Bitcoin mining pools allow us to identify cryptomining hubs—countries and subnational regions in China and the US with a sizable share of global mining activity. Until its 2021 ban, China dominated the Bitcoin mining industry, with a global market share of over 50%. Even within China, nearly 90% of Bitcoin mining was concentrated in four energy-rich western provinces: Xinjiang, Sichuan, Yunnan, and Inner Mongolia. In May 2021, China suddenly banned cryptomining nationwide, citing concerns over its carbon footprint.[3] Mining activity collapsed after the ban—completely to zero in July and August 2021, before rebounding somewhat thereafter. We estimate the impact of China's ban using a difference-in-difference (DiD) design, comparing electricity consumption and generation in mining versus non-mining provinces, before versus after the ban.

The ban reduced monthly energy consumption in each mining province by 1,170 gigawatt hours (GWh), about 5% of the pre-ban level. Across the four mining provinces, the 4,679 GWh reduction amounts to 0.59% of China's total monthly consumption, comparable to the monthly electricity use of Portugal or the US state of Massachusetts. Monthly fossil generation in each mining province fell by an average of 953 GWh, about 5.5% below pre-ban levels. These estimates imply that the ban reduced China's monthly carbon emissions by 3.8 million metric tons, about 0.35% of China's total emissions.

The ban reshaped both the fuel mix and geography of power generation in China. Fossil generation declined in three of the four mining provinces—including in Yunnan, where over 80% of generation comes from renewables. By contrast, we find little evidence that the ban decreased wind, solar or hydropower generation. Our results imply that fossil fuels were the marginal power source for cryptomining in China. With cryptomining demand curtailed, energy-abundant mining provinces—already net exporters of electricity before the ban—increased exports of surplus generation to other provinces. Monthly interprovincial electricity exports from mining provinces grew by 1,679 GWh, a 14% increase.

[3] The ban, discussed in section 2.2, was publicly announced and covered in the media, e.g., see this article. This policy was specific to cryptomining, as crypto trading had already been restricted in prior years.

This spike was driven by Sichuan and Yunnan, aided by new hydropower capacity from the opening of two large hydropower dams.[4] The ban thus did more than cut energy demand: it shifted generation away from fossil fuels and redirected surplus power in mining provinces.

While China's ban reduced domestic emissions, it triggered a global relocation of mining activity. International trade data allow us to directly trace this migration. Using a DiD design, we find that the ban boosted Chinese exports of cryptomining equipment—such as mining rigs and hashboards—to the US, the largest Bitcoin mining hub after China. US import data show a similar pattern: imports of cryptomining equipment, from China and other countries, increased substantially after the Chinese ban relative to similar electronics products. Furthermore, these cryptomining inputs flowed primarily to US states with established mining operations, like Texas and Georgia. Consistent with this relocation, we find that Bitcoin mining activity increased significantly in the US after the ban. This is a rare example of a dirty industry relocating to a developed country in response to environmental regulation in a developing country—the opposite of the North-South pollution displacement discussed in the literature (Tanaka et al., 2022).

The influx of mining activity increased US energy use. Using a DiD design, we find that the ban led to higher commercial and industrial electricity use in US cryptomining states. Residential electricity consumption in mining states did not change and, if anything, declined slightly after the ban. The additional electricity demand was primarily met by fossil fuels: cryptomining states increased fossil generation after the ban, while renewable generation remained unchanged. The evidence suggests that, as in China, fossil fuels were the marginal energy source powering US-based cryptomining.

To better understand the US generation response, we analyse daily operation data for over 1,000 fossil-fuel power plants. We find that the increase in electricity generation in US cryptomining states was driven by old coal-fired plants, which were being phased out in non-mining states. By contrast, the ban did not affect generation or operating hours at gas and newer coal facilities. Taken together, our results suggest that China's ban increased electricity consumption in the US, and this demand was met by the least efficient and most carbon-intensive energy sources.

We estimate the combined effect of China's ban by jointly analysing subnational energy use in Chinese provinces and US states. The ban led to a net 0.4% drop in electricity consumption and a 0.5% decrease in fossil generation over the subsequent two years, as

[4] Sichuan's 10-GW Wudongde and Yunnan's 16-GW Baihetan both started generating power in June 2021.

reductions in China outweighed increases in the US. We estimate that leakage due to the relocation of mining activity attenuated the global impact of China's ban by 31-37%.

Yet banning carbon-intensive digital industries is often infeasible or economically unwise. An alternative decarbonisation strategy is to encourage firms to adopt cleaner technology. In the second part of the paper, we evaluate the impact of Ethereum's transition from PoW to Proof-of-Stake (PoS), a more energy-efficient consensus mechanism. PoS selects transaction validators based on the cryptocurrency they stake as collateral rather than through computational work, and is estimated to use 99.95% less energy than PoW (Asif and Hassan, 2023). For this reason, policymakers—including the White House and the European Commission—have exhorted cryptocurrencies to adopt PoS (Bateman, 2022).

Ethereum switched completely from PoW to PoS at exactly 2:45am EST on 15 September 2022. Using hourly data on US electricity consumption and a regression discontinuity in time (RDiT) design (Hausman and Rapson, 2018), we estimate that this voluntary clean technology adoption reduced hourly electricity consumption by between 6.8 and 16.6 GWh (1.3-3.2% of the pre-transition mean), depending on the bandwidth used. The decline was larger in states and balancing authority regions with more Ethereum nodes, a proxy for pre-transition mining intensity.

Miners responded to Ethereum's transition by redeploying their equipment. Ethereum was designed to be mined with multi-purpose Graphics Processing Units (GPUs), whereas Bitcoin and some other cryptocurrencies can only be profitably mined with specialised Application-Specific Integrated Circuits (ASICs). Just after Ethereum's transition, daily hashrates for other GPU-mined cryptocurrencies (e.g., Ethereum Classic, Ravencoin, Ergo) increased by 0.3-0.6 standard deviation—among the largest daily spikes in their histories. By contrast, we observe almost no change in mining activity for ASIC-dedicated coins such as Bitcoin. The redeployment of energy-intensive GPU inputs away from Ethereum toward other GPU-mined PoW cryptocurrencies diluted the impact of Ethereum's transition by about 30%. Our findings reveal a second way in which firms undermine non-comprehensive decarbonisation policies: by leaking carbon-intensive production factors to unregulated dirty activities. To our knowledge, there is comparatively little evidence on this form of leakage.

In sum, two major policies to decarbonise cryptomining—a national ban in the largest market and clean technology adoption by its second-biggest platform—were only partly effective, as miners relocated or repurposed equipment. Our findings underscore the challenge of decarbonising industries that use mobile, multi-purpose production factors. Similar concerns apply to other emerging computation-heavy industries. While AI data centres may be less mobile than cryptomining farms, their emissions are also footloose, as cloud routing allows firms to reallocate computing demands across facilities worldwide. AI data centres also use versatile hardware that can be redeployed across applications, complicating efforts to curb emissions. Moreover, both cryptomining and AI require round-the-clock electricity, which is typically supplied at the margin by dispatchable power sources like fossil fuels (Joskow, 2011; Borenstein, 2012; Gowrisankaran et al., 2016).

Contribution to the literature. Our paper relates to three areas of research. First, we add to a growing literature that evaluates decarbonisation policies, including emissions trading schemes (Greenstone et al., 2025; Colmer et al., 2025), carbon offsets (Calel et al., 2025), carbon taxes (Andersson, 2019; Klenow et al., 2024), border tariffs (Farrokhi and Lashkaripour, 2025; Clausing et al., 2025), and regulation of dirty industries (Hansen-Lewis and Marcus, 2025; Hsiao, 2026). A central theme is that firms respond strategically to environmental regulation, causing pollution displacement and carbon leakage (Eskeland and Harrison, 2003; Hanna, 2010; Gibson, 2019; He et al., 2020; Zou, 2021; Hong and Chen, 2026). Leakage may be especially difficult to prevent in computation-heavy digital industries, which have mobile, multi-purpose production factors—yet there is limited empirical evidence on how to decarbonise such activities (Dugoua and Moscona, 2025). While most studies focus on North-South pollution displacement triggered by regulation in rich countries (Davis, 2008; Tanaka et al., 2022; Levinson, 2023), we document a rare case of South-North displacement. As developing countries adopt more ambitious environmental policies, such spillovers may become increasingly important.

Second, we contribute to a burgeoning literature on the economics of cryptocurrencies (Halaburda et al., 2022; Biais et al., 2023; John et al., 2022; Makarov and Schoar, 2022).[5] While several studies describe the link between cryptomining and electricity markets (Liu and Tsyvinski, 2021; Halaburda and Yermack, 2023), most estimates of the energy intensity of mining rely on engineering models (Stoll et al., 2019) rather than actual electricity consumption.[6] Three recent papers are particularly related to ours. Papp et al. (2023) shows

[5] Research focuses on cryptocurrency foundations (Capponi et al., 2023; Sockin and Xiong, 2023; Budish, 2024), their function as currencies (Alvarez et al., 2022; Jermann and Xiang, 2025), investor behaviour and trading patterns (Makarov and Schoar, 2020; Cong et al., 2023; Benetton and Compiani, 2024; Lin et al., 2025), and household responses to crypto market fluctuations (Aiello et al., 2023; Cong et al., 2024).

[6] Krause and Tolaymat (2018), Goodkind et al. (2020), and Gallersdörfer et al. (2020) estimate that Bitcoin mining consumes 46 TWh of electricity and generates 22 Mt of carbon emissions. Jones et al. (2022) finds that Bitcoin's carbon footprint has risen over time. These papers rely on engineering models that make

that Bitcoin mining incentives affect carbon emissions using daily data from an integrated miner-cum-generator in Pennsylvania. Benetton et al. (2023) shows that cryptomining pushes up electricity prices, crowding out other electricity users and lowering local economic growth. Lu et al. (2025) find that Chinese cryptominers relocate to hydro-abundant provinces during the wet season to take advantage of cheaper electricity. However, none of these papers study policies to decarbonise cryptomining.

To our knowledge, ours is the first paper that evaluates efforts to reduce the energy use of computation-heavy activities—highlighted by Dugoua and Moscona (2025) as an important topic for future research. We study two such policies: China's cryptomining ban and Ethereum's transition to clean PoS technology. While both reduced the energy footprint of their targeted activities, their global effects were diluted by distinct forms of leakage, as miners relocated operations after China's ban and redeployed carbon-intensive equipment after Ethereum's transition. Our findings have implications for regulating emerging digital goods, as most pricing- and standards-based energy-efficiency policies, such as the EU's Carbon Border Adjustment Mechanism, were designed for physical goods, where flows are easier to track.

Third, we contribute to the literature on electricity markets. Prior work emphasizes that renewables are imperfect substitutes for dispatchable fossil-fuel generation because they cannot reliably adjust output to meet demand without large-scale storage (Joskow, 2011; Borenstein, 2012; Gowrisankaran et al., 2016; Butters et al., 2025). This distinction is especially relevant for computation-intensive industries such as cryptomining, which require continuous, round-the-clock electricity and therefore place persistent demand on the grid (Graff Zivin et al., 2014; Borrero et al., 2023). We find that the marginal generators supplying cryptomining are primarily fossil-fuelled, even in regions with substantial renewable capacity. The growth of computation-intensive industries could thus reinforce the role of dispatchable fossil generation at the margin, even as renewable capacity expands.

The remainder of this paper is organized as follows. Section 2 provides background on cryptomining and describes the institutional context of the policies we study . Section 3 describes the data. Section 4 examines the domestic impacts of China's mining ban and Section 5 presents evidence of its global spillovers. Section 6 evaluates the effectiveness of Ethereum's clean technology adoption. Section 7 discusses external validity and concludes.

assumptions about the energy efficiency of mining equipment and the *average* electricity mix of mining locations. By contrast, we analyse electricity consumption in China and the US and exploit natural experiments to estimate cryptomining's energy intensity.

2 Background & Institutional Context

2.1 Cryptocurrencies and cryptomining

A cryptocurrency is a digital currency whose transactions are verified and secured by a decentralised system based on cryptography. To maintain transaction records, cryptocurrencies rely on blockchain technology (Halaburda et al., 2022). By 2023, there were 9,000 cryptocurrencies with a market capitalisation totalling US$1 trillion, but a few cryptocurrencies dominated the market (CoinMarketCap, 2024). Bitcoin, the first and largest cryptocurrency, had a 51% market share, while Ethereum, the second largest, had 17%.

Cryptocurrencies rely on a decentralised consensus mechanism to verify transaction blocks and update the blockchain. In the most widely used consensus mechanism, Proof-of-Work (PoW), a transaction block is secured by a cryptographic hash that is generated when a miner solves a mathematical puzzle. The first miner to solve the puzzle wins the right to update the ledger with a new transaction block and earns a cryptocurrency reward. Since puzzles are solved by brute-force trial-and-error, miners invest heavily in computing power. While some cryptocurrencies (e.g. Bitcoin) can only be efficiently mined with specialised hardware—Application-Specific Integrated Circuits (ASICs)—other cryptocurrencies (e.g. Ethereum) were designed to be mined with general-purpose Graphics Processing Units (GPUs). Whether employing ASICs or GPUs, the PoW consensus mechanism is highly energy-intensive, with engineering estimates suggesting that Bitcoin mining consumes more electricity than Pakistan or the Netherlands (Chamanara et al., 2023).[7]

Because energy is such an important input, miners seek locations with abundant, cheap, and reliable power—a key reason China dominated the global Bitcoin mining industry before its 2021 ban. Cryptomining's energy intensity has drawn concerns about its carbon footprint (Foteinis, 2018; Chamanara et al., 2023), which some miners have sought to allay by locating near hydro or wind power plants.[8] However, even miners using renewable power may indirectly increase fossil generation. By boosting electricity demand, miners may displace other consumers, forcing them to use fossil-generated power or pay more (Benetton et al., 2023; Bushnell, 2024). Moreover, cryptomining operations typically run continuously, requiring round-the-clock electricity. Meeting this demand requires gener-

[7] However, modelling assumptions make engineering estimates vary widely. The Crypto Carbon Ratings Institute estimates that Bitcoin consumes 14,700 GWh annually, whereas the Cambridge Bitcoin Energy Consumption Index's estimate is 18,300 GWh with a wide range between 9,500 and 394,000 GWh.

[8] See this example in Texas and the broader discussion in Stoll et al. (2023).

ators that supply power on demand—typically dispatchable fossil-fuel plants rather than intermittent renewables. Increased cryptomining demands can thus raise fossil generation at the margin, even in regions with substantial renewable capacity.

Cryptomining has been blamed for overloading grids and causing blackouts, prompting several countries—including Iran and Russia—to introduce mining bans.[9] By far the most consequential of these restrictions was China's 2021 ban on cryptomining.

2.2 China's ban on cryptomining

The cryptocurrency industry expanded rapidly in China during the 2010s. The country opened its first Bitcoin exchange, BTCChina, in 2011 and cryptocurrency transactions increased soon after (Feng, 2021). Bitmain, still the world's leading manufacturer of cryptomining equipment, was established in Beijing in 2014. By 2018, Bitmain alone produced 70% of the rigs used to mine Bitcoin globally (De Vries, 2018; Sharma, 2023), and 77% of global Bitcoin mining occurred in China (Kaiser et al., 2018).

China first introduced restrictions on the crypto industry in 2017, imposing bans on cryptocurrency transactions, currency exchange between cryptocurrencies and the yuan, and initial coin offerings (Borri and Shakhnov, 2020; Chen and Liu, 2022). However, none of these regulations covered or directly affected cryptomining.

The Chinese government began to restrict cryptomining in 2021, ostensibly to reduce carbon emissions and free up electricity supply (Pan, 2021). In February 2021, Inner Mongolia's provincial government published draft guidelines to ban new cryptomining projects, but existing cryptomining operations were not impacted and were allowed to continue. On 21 May 2021, the Financial Stability and Development Committee of the State Council, China's highest administrative authority, released a statement committing to "crack down on Bitcoin mining and trading activities".[10] The response was swift: provincial governments quickly passed their own regulations, and social network Weibo and search engine Baidu moved to censor search results related to cryptocurrency.

On 25 May 2021, Inner Mongolia's provincial government released eight measures to "resolutely Crack Down on and Punish Virtual Currency Mining Behavior".[11] On 9 June 2021, officials in Xinjiang ordered cryptomining activities at industrial plants to shut down.[12] On 12 June 2021, the Yunnan Energy Bureau said it would cut power supply to

[9] See press examples of cryptomining-induced power outages in Kosovo, Iran and Russia.
[10] The Committee's statement is here and press coverage of it is here.
[11] The full government order is available here.
[12] This article describes the Xinjiang government's crackdown on cryptomining.

cryptominers and promised to shut down any firm in violation of the new rules. On 18 June 2021, the Sichuan Provincial Development and Reform Commission and the Sichuan Energy Bureau issued a joint notice ordering local electricity companies to immediately "screen, clean up and terminate". The notice also ordered local electricity companies to immediately stop supplying power to cryptomining projects and banned local authorities from approving new mining projects.[13]

Thus, between May and June 2021, the governments of China's four major cryptomining provinces—Xinjiang, Sichuan, Inner Mongolia, and Yunnan—all issued strict orders to ban cryptomining activity. As such, we use May 2021 as the timing of China's ban, though treating June 2021 as the policy timing yields similar results.

2.3 Ethereum's clean technology adoption

The two most popular consensus mechanisms used by cryptocurrencies are Proof-of-Work (PoW) and Proof-of-Stake (PoS). Under PoW, used by 60-65% of the market (including Bitcoin), miners compete to solve cryptographic puzzles. The competition rewards raw computational power, requiring miners to run vast quantities of specialised hardware. Proof-of-Stake (PoS), used by 20-25% of the market, dispenses with this competition entirely: validators are selected probabilistically in proportion to the cryptocurrency they pledge as collateral, eliminating the need for energy-intensive computation. As a result, PoS is estimated to use 99.95% less energy (Asif and Hassan, 2023) than PoW. For this reason, the European Commission and White House have urged the cryptocurrency industry decarbonise by replacing PoW with a cleaner consensus mechanism (Bateman, 2022).

Ethereum was launched in 2015 using PoW technology, but its founder envisioned an eventual transition to PoS. In 2020, Ethereum took its first step toward adopting PoS, implementing the Beacon Chain, a parallel blockchain that allowed developers to test and stabilise PoS, setting the foundation for Ethereum's full transition in 2022.

After several delays, Ethereum merged its main network with the Beacon chain on 15 September 2022, at 2:45am EST. This event, known as The Merge, marked Ethereum's complete transition to PoS and the end of Ethereum's mining. Our data confirm that mining activity collapsed to zero on the event date (Figure A.1). Before the transition, Ethereum mining consumed as much energy as Paraguay or Ghana. Ethereum's adoption of PoS had significant potential to decarbonise cryptomining.[14]

[13] Yunnan's restrictions are described here, while this article details Sichuan's ban on cryptomining.

[14] This website describes The Merge. Ethereum's energy use is benchmarked here.

3 Data

3.1 Cryptomining activity

Bitcoin mining. We obtain data on Bitcoin mining activity from the Cambridge Centre for Alternative Finance (CCAF), a standard industry source that provides ”the most widely accepted estimates on the energy consumption of Bitcoin and Ethereum” (Chamanara et al., 2023). CCAF's data are widely used by government agencies, including the US Energy Information Administration and the International Energy Agency.[15] The data provide monthly Bitcoin hashrates for 77 countries between September 2019 and January 2022.[16] We use these data to identify six major mining countries—China, the US, Russia, Kazakhstan, Iran, Malaysia and Canada—which jointly account for over 90% of global mining activity.

CCAF also reports subnational hashrates for China and the US, which we use to identify cryptomining hubs in both countries.[17] In China, four provinces—Xinjiang, Inner Mongolia, Sichuan, and Yunnan—collectively account for about 90% of the national hashrate. In the US, the major mining states are Texas, Georgia, New York, Kentucky, and California, which jointly account for 75% of the US hashrate. Unlike the other four states, we did not find press reports of large mining facilities in California. We therefore show that all our results are robust to excluding California from the list of US mining hubs.[18]

To compile its data, CCAF partners with several large Bitcoin mining pools—groups of miners who combine computational power to exploit economies of scale and to smooth lumpy mining revenues. Pools observe the IP addresses of miners connecting to their servers and report aggregated data on miners' geographical distribution via a privacy-preserving API. The CCAF approach relies on two key assumptions: (1) the participating pools, which comprise 32–38% of total network hashrate, are representative of global mining activity, and (2) IP addresses accurately reflect where mining occurs.

We perform two validation exercises to assess how spatially representative CCAF's data are, benchmarking it against public, non-manipulable information on total, network-

[15]The CCAF's data is used by the US EIA in its analyses of US cryptocurrency mining electricity demand (see here), by the IEA in its Electricity Market Reports (see here), and by the White House Office of Science and Technology in its 2022 report on climate and energy implications of crypto-assets in the US (see here).

[16]The hashrate measures cryptomining's computational power. It indicates the number of cryptographic calculations (hashes) miners perform each second when solving PoW puzzles.

[17]China's subnational hashrate data are only available until June 2021, while for the US we observe a snapshot in December 2021.

[18]While CCAF shows a high hashrate for California, some of this could reflect proxy servers.

wide mining activity. First, CCAF mining activity closely tracks month-to-month fluctuations in the global network hashrate, measured independently using data from Coinbase, a major cryptocurrency exchange (figure A.2). The tight co-movement suggests that the CCAF data capture overall trends in mining activity. Second, CCAF's estimate of China's pre-ban hashrate closely aligns with the total decline in the network hashrate following China's ban, supporting the accuracy of CCAF's spatial distribution data.

Next, we consider the assumption that IP addresses reflect actual cryptomining locations. Attempts to obscure location using proxy servers or virtual private networks hurt mining revenues, as they increase network latency, reducing a miner's probability of winning the race to solve cryptographic puzzles (Braiins, 2020). Thus, miners have strong incentives to connect to nearby servers. Moreover, our empirical strategy does not exploit fine-grained variation in mining intensity; instead, we use a binary measure, classifying locations as major mining hubs or non-mining areas, which makes the analysis less sensitive to moderate location mismeasurement. While CCAF's data may not precisely capture Sichuan's or Texas' exact hashrate, we are unlikely to misclassify a major mining hub as a non-mining location. Given the scale of our geographic units (countries, Chinese provinces and US states), we believe the reported mining locations are broadly accurate. Any measurement error might attenuate our estimates toward zero.

Figure A.3 shows the global distribution of Bitcoin mining prior to the Chinese ban, with China being the dominant player followed by the US. Figure A.4 shows the distribution within China, by season. During the wet summer months, Sichuan and Yunnan, provinces with significant hydropower capacity, account for 63% of China's total hashrate. In the dry winter months, their share drops to 30%. Such seasonal patterns are noted in media reports and by other researchers (Lu et al., 2025), further validating our data.

Mining of other PoW cryptocurrencies. Given limited information on the locations of non-Bitcoin miners, we collect high-frequency data on total mining intensity for other PoW cryptocurrencies (such as Ethereum, Ethereum Classic, Ravencoin and Ergo). We compile the daily hashrate and closing price of cryptocurrencies over the period 2021-2023 from platforms such as CoinMetrics, CoinWarz, and CoinMarketCap. In addition, we scraped the locations of all Ethereum validator nodes prior to the platform's transition to PoS.

International trade in cryptomining equipment. Cryptomining requires dedicated hardware to run mining algorithms and China is by far the biggest manufacturer of such equipment. To study the relocation of mining equipment after China's ban, we compile data on exports from China's General Administration of Customs. This data contains information on monthly export value by destination country for each 8-digit Harmonized System (HS) product code. We identify HS codes for the most popular cryptomining machines (e.g., Antminer) and accompanying or embedded hashboards reported on the website of Bitmain, the world's dominant mining rig manufacturer (Bitmain, 2022). This data enables us to compare exports of cryptomining inputs against those of very similar products.

Anecdotal evidence suggests that mining activity relocated primarily to the US after China's ban.[19] To test this, we collect US import data on computing—including cryptomining—equipment from the Census Bureau. To identify cryptomining imports, we use products cited in a Customs and Border Protection tariff ruling, which assigned a 10-digit HS code to two cryptomining machine brands (US CBP, 2018). We also identify products whose HS codes share the first 6-digits of cryptomining equipment exported from China (see Table A.1).

3.2 Electricity consumption and generation

Electricity inputs. For each Chinese province, we obtain monthly data between January 2018 and July 2023 on electricity consumption, generation, and transmission to other provinces. Consumption and inter-province transmission come from the Wind Economic Database, whereas generation by source are from China's National Bureau of Statistics and Electricity Statistical Yearbook. For the US (and for the same period unless noted), we collect data on (i) monthly state-level electricity consumption by sector and generation by source from the EIA; (ii) daily electricity generation for 1,250 active fossil-fuel power plants from the Clean Air Markets Program; and (iii) hourly electricity consumption by balancing authority from the EIA's Hourly Electric Grid Monitor (2021-2023). At the country level, we compile monthly electricity consumption and source-wise generation for 40 OECD countries from the IEA, and supplement with data series on Kazakhstan, Russia, and Malaysia from CEIC and Jabatan Perangkaan Malaysia.

Weather. Since weather is an important determinant of energy use, we compile hourly data on ambient temperature, precipitation, dew point temperature (humidity), and wind speed at weather station level from the National Oceanic and Atmospheric Administration (NOAA). For subnational analyses, we average daily readings across all stations within a

[19] E.g., see press articles on the relocation of cryptomining here and pollution displacement here.

province or state, and aggregate to the monthly level.[20] For the power plant-level analysis, we construct plant-by-day weather variables by taking the inverse-distance weighted average across all NOAA stations within 50 miles of each plant.

4 Direct effects of China's ban on cryptomining

4.1 Empirical strategy

To investigate the impact of China's ban on cryptomining, we estimate a standard difference-in-differences (DiD) specification:

$$Y_{it} = \beta MiningProvince_i \times PostBan_t + X_{it}^{'}\Gamma + \alpha_{i(m)} + \alpha_t + \epsilon_{it} \tag{1}$$

where Y_{it} is an outcome of interest (e.g., electricity use) for province i in month-of-sample t. $MiningProvince_i$ is an indicator for the four major cryptomining provinces (Inner Mongolia, Xinjiang, Sichuan, Yunnan), which we identify using pre-ban mining activity. As explained in section 2.2, $PostBan_t$ takes value 1 from May 2021 onwards. The coefficient of interest is β. We include (i) province fixed effects $\alpha_{i(m)}$ to control for differences across provinces, allowing these to vary by season via month-of-year interactions;[21] and (ii) month-of-sample fixed effects α_t to control for factors that affect all provinces in a particular month, e.g., Bitcoin price fluctuations. We further control for (iii) weather (temperautre, precipitation, humidity and wind speed)[22], and (iv) province-specific linear trends. Standard errors are clustered at the province level.

To test the parallel trends assumption, we estimate a dynamic DiD specification:

$$Y_{it} = \sum_{k \neq -1} \beta_k MiningProvince_i \times \mathbb{1}(Time_t = k) + X_{it}^{'}\Gamma + \alpha_i + \alpha_t + \epsilon_{it} \tag{2}$$

where $\mathbb{1}(Time_t = k)$ is indicator for whether month t is $k \in [-12, 12]$ months away from the

[20] Because NOAA precipitation records are largely missing for China, we complement with monthly precipitation at 0.25-degree grid resolution from NASA's GLDAS Version 2 Data product, averaging across all grid cells within each province.

[21] For instance, this accounts for heating demand in the winter in the colder north and expansions in hydropower generation during the rainy season in provinces like Sichuan and Yunnan.

[22] Specifically, the weather controls are the proportion of days in a month in which a province's daily mean temperature falls into each of 5°C-wide bins, mean precipitation and its square term, mean dew point depression, and mean wind speed

ban.[23] For robustness and to improve precision, we also implement a synthetic difference-in-differences (SDiD) estimator, which weights control units to approximate treated units in the pre-period (Arkhangelsky et al., 2021).[24]

4.2 Impacts on electricity consumption

The ban was effective at shutting down cryptomining in China. The Bitcoin hashrate of China-based miners declined rapidly in May 2021, continued to decrease in June 2021, and fell to zero in July and August 2021 (Figure A.5). Although some mining resumed later in the year—in contravention of the ban—mining activity remained well below its pre-ban level. The ban thus offers a valuable setting to examine the energy market effects of cryptomining.

Baseline results. We find that the ban decreased electricity consumption. Dynamic DiD estimates in figures 1a and 1b show support the parallel trends assumption. Relative to non-mining provinces, monthly electricity consumption in each mining province fell by 1,170 GWh, or 5% of the pre-ban mean (table 1, column 1). Across four major mining provinces, the ban reduced consumption by 4,679 GWh, nearly 0.59% of China's total monthly electricity consumption. For perspective, this is comparable to the monthly electricity use of Portugal or the US state of Massachusetts, and larger than the monthly consumption of 160 countries.

The ban led to large, statistically significant declines in electricity consumption in three of the four mining provinces (table 1, column 2). Only Sichuan shows no decrease in energy consumption. This could be because mining went underground: Sichuan's network of smaller dams may have enabled miners to access off-grid hydropower hidden from regulators; also Sichuan's government was initially more lenient at enforcing the ban.[25]

[23] We exclude $k = -1$ for normalisation and group months outside this window.

[24] Unit weights ω_i and time weights λ_t are constructed so that the synthetic counterfactual exhibits parallel trends to treatment provinces in the pre-period. Estimated weights $\hat{\omega}_i$ and $\hat{\lambda}_t$ are then applied to the DiD regression to estimate the causal impacts of the ban. Following Kranz (2022), we estimate Γ by regressing Y_{it} on X_{it} and the two-way fixed effects using pre-treatment observations. The SDiD procedure is applied to the adjusted outcome $Y_{it}^{adj} = Y_{it} - X_{it}'\hat{\Gamma}$ to obtain $\hat{\beta}^{SDiD}$. To estimate dynamic coefficients, we calculate the outcome differences between treated units and synthetic controls at each period compared to pre-treatment weighted average, using optimal time weights $\hat{\lambda}_t$ (Clarke et al., 2023). The covariance matrix uses cluster bootstrapping at the province level with 1000 replications.

[25] Anecdotally, miners may have believed that the ban's enforcement would be weaker in Sichuan given its extensive hydropower, consistent with its provincial government taking one month to issue strict instructions after the State Council's "crackdown" statement (see here and, on off-grid power access, see here).

Robustness. Our results are robust to alternative specifications. SDiD estimates are similar, albeit slightly smaller and more precise (table 1, column 3). We also implement a staggered DiD regression where treatment timing varies slightly by province, finding similar results (table A.4).

As with any DiD design, it is important to investigate whether our effects could be driven by concurrent events or policy changes. We consider two potential confounders. First, COVID-19: if mining provinces had stricter mobility restrictions in 2021, these could lower economic activity and account for lower electricity consumption. However, we show that mining provinces did not have more stringent lockdown policies or lower local economic activity, as proxied by night-time luminosity (Table A.2). Consistent with this, we obtain similar estimates after controlling for COVID-19 lockdown stringency or night-time luminosity at the province-by-month level (table A.3, columns 2 and 3).

Second, China's "dual control" policy in 2016 set energy intensity and consumption targets for provincial governments, to be assessed and updated every five years. In June 2021, nine provinces (including Yunnan) received a warning notice for underperforming on their targets.[26] Our results are robust to controlling for whether a province was flagged for poor performance (table A.3, column 4), as well as controlling for COVID-19 stringency, nighttime light intensity, and dual-control warning together (column 5).

The ban was also unexpected. As noted, it was announced on 21 May 2021 and implemented nationwide shortly after. Consistent with this, we find evidence of no pre-trends in electricity consumption (figure 1a) and, as shown subsequently, in exports of cryptomining equipment (figure A.10) or Bitcoin hashrates (figure 2). If some miners did anticipate the ban, our estimates should be interpreted as a lower bound.

4.3 Impacts on electricity generation

Having shown that the ban reduced electricity consumption in mining provinces, we examine impacts on electricity generation.

Fossil generation. Figures 1c and 1d show that the ban decreased fossil generation. Our baseline DiD estimates indicate that monthly fossil generation fell by 953 GWh in each

[26] Introduced as part of the 2016 13th Five-Year Plan, the dual-control policy's goals were reinforced under the March 2021 14th Five-Year Plan. On 3 June 2021, the National Development and Reform Commission issued a "level 1" (highest risk) warning notice to Qinghai, Ningxia, Guangxi, Guangdong, Fujian, Xinjiang, Yunnan, Shaanxi, and Jiangsu.

mining province, or 5.5% of the pre-ban mean (table 2, column 1). Fossil generation declined significantly in three out of four mining provinces: even Yunnan, where over 80% of electricity comes from renewable sources (Liu et al., 2019), experienced a 903 GWh fall in monthly fossil generation. Our findings are robust to controlling for potential confounders such as COVID-19 restrictions, local economic activity, and dual-control policy warnings (table A.3, panel B). Across the four mining provinces, our estimates imply 3,812 GWh lower monthly fossil generation and 3.9 million ton lower associated carbon emissions—about 0.9% of China's total fossil generation and 0.35% of its total emissions.[27]

Renewable generation. By contrast, the evidence suggests that the ban did not decrease renewable generation in mining provinces. There is no discernible change in wind and solar generation after the ban (figures A.6c-A.6f). Our baseline DiD estimates similarly show a null effect (table 2, columns 3-4).

Hydropower generation in mining provinces actually increased after the ban (figures A.6a-A.6b), driven by Sichuan and Yunnan (table 2, column 2). However, we do not believe this is an effect of the ban, but rather reflects the opening of two major hydropower plants—16-GW Baihetan and 10-GW Wudongde—in Sichuan and Yunnan in June 2021, and a smaller dam (Altash) in Xinjiang in August 2021. The increased hydropower capacity is large enough to fully account for the generation surge.

Several robustness checks show that the decline in fossil generation is not simply an artefact of greater hydropower capacity. First, we control directly for each province's time-varying hydropower capacity and our fossil generation results remain similar (table A.5). Second, we examine the ban's effect separately by province and season. We find reductions in fossil generation in Inner Mongolia, Xinjiang and Yunnan in both wet and dry months, and in Sichuan during the wet season (Figure A.7). Moreover, in the coal-heavy provinces of Xinjiang and Inner Mongolia, which experienced little change in hydropower capacity, we see large and significant fossil generation declines, and similar effects in both seasons (Figure A.7). The robust, stable decline in fossil generation in Inner Mongolia and Xinjiang—where new hydropower capacity is not a confounding factor—supports the conclusion that the ban meaningfully reduced fossil generation in mining provinces.

Taken together, our interpretation is that the ban decreased fossil generation, but had a limited impact on renewable generation. Our findings suggest that fossil fuels powered

[27] China's monthly pre-ban fossil generation is 429,132 GWh . We convert to carbon emissions using the US EIA (2023) factor for coal generation (1,023 $kgCO_2$/GWh), since China's fossil generation is primarily coal. This may be an underestimate if the emissions factor of Chinese coal plants exceeds that in the US.

the marginal generators supplying Chinese cryptominers. Our empirical estimates challenge the claim that, by locating near renewable sources, cryptominers do not contribute to fossil fuel use. Rather, even miners who rely primarily on renewables may displace other consumers who then use fossil-generated power.

Total generation and electricity exports. Although the ban reduced electricity consumption in mining provinces, we see no change in total generation (figures A.8a and A.8b). The DiD estimate is small (table 2, column 5): with 95% confidence, we can rule out total generation declines of more than 3.7%. To close the loop, we examine data on inter-province electricity exports. Even before the ban, the energy-abundant mining provinces were substantial net exporters, with each mining province exporting on average 11,705 GWh per month, or 35% of their total generation.

We find that mining provinces increased their net exports of electricity after the ban (figures A.8c and A.8d). On average, the ban raised each mining province's monthly electricity exports by 1,679 GWh, a 14% increase over the pre-ban mean (table 2, column 6). Standard DiD and SDiD estimates are again similar (panel B). The export surge was most pronounced for Sichuan and Yunnan, due in part to the opening of the new dams—though Inner Mongolia, which experienced no change in generation capacity, also increased its electricity exports. The ban thus changed the fuel mix and geography of power generation in China: less fossil generation, and more electricity exports from the mining provinces.

Overall, our results indicate that China's ban was reasonably effective at curbing domestic energy use and carbon emissions from cryptomining. Mining activity fell drastically, reducing China's total electricity consumption by 0.59% and total fossil generation by 0.9%—reductions that are economically significant in magnitude.

5 Global spillovers of China's cryptomining ban

5.1 International relocation of cryptomining

China's sudden ban left cryptominers with large quantities of specialised equipment that could no longer be used domestically. To test whether the ban shifted mining activity abroad, we turn to international trade data.

5.1.1 Chinese exports of cryptomining equipment

Raw data suggests that China raised its exports of cryptomining machines to other major cryptomining countries compared after the ban (Figure A.9a). To test this formally, we estimate a triple difference regression, which compares the differential change in Chinese exports to mining versus non-mining countries for cryptomining equipment compared to similar products in the same narrowly defined industry, before versus after China's ban:

$$Y_{ijt} = \beta MiningEquipment_j \times MiningCountry_i \times PostBan_t + \alpha_{ij} + \alpha_{it} + \alpha_{jt} + \epsilon_{ijt} \quad (3)$$

where Y_{ijt} denotes Chinese exports of HS8 product j to destination (country) i in month t. This demanding specification includes destination-by-product, destination-by-month, and product-by-month fixed effects. Destination-by-month accounts for any confounding factor that affects all Chinese exports to particular countries (e.g., a trade war), whereas product-by-month controls for factors that affect demand for a product across destinations (e.g., cryptocurrency prices, technology shocks). In a variant of this specification, we explore separate impacts on the US and on other mining countries.

We find that Chinese exports of cryptomining equipment surged after the ban, destined for the US (figure A.10a) and, to a lesser, for other mining countries (figure A.10b). Our triple difference estimates show that the ban increased China's cryptomining equipment exports to mining countries by 30% relative to similar products in the same HS 8471xxxx category (Table 3, column 1).[28] Column 2 confirms that this effect is driven by higher exports to the US. A doubly robust triple difference procedure (Ortiz-Villavicencio and Sant'Anna, 2025) shows similar results (Table 3, panel B).

5.1.2 US imports of cryptomining equipment

US import data offer further evidence that the cryptomining industry relocated after the ban. Raw data plots suggest that US imports of cryptomining machines increased relative to those of similar products after the ban (Figure A.9b). To test this formally, we implement the following DiD regression:

$$Y_{jt} = \beta MiningMachine_j \times PostBan_t + \alpha_j + \alpha_t + \epsilon_{jt} \quad (4)$$

where Y_{jt} refers to US imports of HS10 product j in month t.

[28] Examples of similar products includes scanners (HS8 code: 84716050), floppy disk drivers (HS8 code: 84717020) and keyboards (HS8 code: 84716071) etc.

We find that US imports of cryptomining machines grew 58% relative to imports of similar products after China's ban, whether directly from China (table A.6, column 1) or from other countries (column 2).[29] Dynamic DiD estimates indicate this response peaked several months after the ban (figure A.11). The evidence suggests that the underlying cause was increased US mining demand rather than simply the offload of idle Chinese mining equipment. Our estimates suggest that the ban increased monthly Chinese cryptomining exports to the US by \$33.8M (table 3) and US cryptomining imports from China by \$39.1M (table A.6). While reassuringly similar, these numbers need not match exactly due to differences in product classification between Chinese export and US import data.

Even within the US, imported mining equipment flowed primarily to established cryptomining hubs such as Texas and Georgia. We estimate a triple difference regression similar to equation (3), comparing US imports of cryptomining equipment vs similar HS6 products by mining vs non-mining states, before vs after China's ban:

$$Y_{ijt} = \beta MiningEquipment_j \times MiningState_i \times PostBan_t + \alpha_{ij} + \alpha_{it} + \alpha_{jt} + \epsilon_{ijt}, \qquad (5)$$

where Y_{ijt} denotes imports of HS6 product j by US state i in month t. As in equation (3), this demanding specification includes state-by-product, state-by-month, and product-by-month fixed effects. State-by-month FEs account for local economic conditions while product-by-month FEs capture common time-varying product-level shocks (e.g., aggregate demand).

We find that cryptomining equipment imports by US mining states grew significantly faster than those of similar products (figures A.10c and A.10d). Table 4 shows that after China's ban, US mining states imported 32% more cryptomining inputs (column 1) and 89% more mining machines (column 2). Increased hashboard imports are less precisely estimated (column 3). Findings are again robust to using the doubly robust estimator cited earlier.

5.1.3 Bitcoin mining activity

Having shown that the ban caused dirty—computation-heavy—physical capital to relocate from China to the US, we now examine a direct measure of cryptomining activity in each country. We compare Bitcoin hashrates in mining vs non-mining countries, before

[29] These could reflect rerouted Chinese exports, as in (Iyoha et al., 2024).

vs after China's ban by implementing the DiD specification:

$$Y_{it} = \beta MiningCountry_i \times PostBan_t + \alpha_i + \alpha_t + \epsilon_{it} \tag{6}$$

where Y_{it} is location i's hashrate in month t and $MiningCountry_i$ is an indicator for the six countries that had significant mining activity before the ban. We include country-by-month-of-year and month-of-sample fixed effects and country-specific time trends.

Figure 2 reports that Bitcoin hashrates increased in established mining countries as a whole after China's ban, with effects growing over time. Leakage was concentrated in the US, where hashrates more than doubled relative to pre-ban levels, with limited change in other mining countries (Table A.7, column 1). This is consistent with our earlier results that cryptomining equipment relocated primarily to the US.

Taken together, our evidence suggests that China's ban caused cryptomining activity to move from energy-abundant Chinese provinces to US states with established cryptomining hubs such as Texas. This is an unusual instance of a pollutive industry relocating to a rich country in response to environmental regulation in a developing country—the opposite of cases documented in the literature, such as Tanaka et al. (2022). Next, we explore how this migration affected electricity consumption and generation in the US.

5.2 The impact of China's cryptomining ban on US energy use

We analyse how the relocation of cryptomining activity affected energy use in the US in two steps. First, we analyse monthly electricity consumption and generation in the over 40 countries for which we have data, and show that US energy consumption increased after the ban. Then, we look within the US, and show that these gains were driven by higher industrial consumption in mining states.

5.2.1 Impact on electricity consumption

US vs other countries. We compare mining vs non-mining countries' electricity use before vs after China's ban, by estimating DiD equation (6) with electricity consumption as the dependent variable.[30] Table A.7, column 2 shows that the ban raised monthly US electricity consumption by 8,034 GWh, or 2.4% of the pre-ban mean, whereas other mining countries show no significant change. This specific estimate seems quite large—in this

[30] We omit China from the sample, as we are interested in the spillover effects on other countries. In section 5.3, we estimate the net impact of China's ban on net China-US electricity use.

country-level panel we do not control for weather—and we turn to subnational US data next. Nevertheless, the estimate is consistent with miners (or mining equipment) relocating primarily to the US in response to China's ban.

Within US: Mining vs non-mining states. We implement a DiD specification similar to equation (1) to compare the electricity use of US mining vs non-mining states before vs after China's ban. Table 5, panel A shows that monthly electricity consumption in each mining state grew by 416 GWh (2.4%), driven by the industrial/commercial sector (+515 GWh, +4.8%). By contrast, residential consumption did not change and if anything declined after the ban (-103 GWh, not significant). Across the five major US mining states, electricity consumption increased by 2,078 GWh per month, about half the monthly energy use of the state of Massachusetts.

These patterns are not driven by outliers: all five mining states show statistically significant increases in total electricity consumption (table 5, panel C), owing to higher commercial and industrial consumption, consistent with an industrial scale being required for competitive cryptomining (Papp et al., 2023). In some US mining states, residential electricity consumption may even have declined after China's ban, consistent with cryptomining crowding out other users (Benetton et al., 2023). Figure A.12 shows that industrial/commercial electricity consumption increased after the ban and continued to grow over time. Furthermore, these conclusions are unaffected by controlling for COVID-19 restrictions, night light intensity, the 2021 Texas freeze, or classifying California as a non-mining state (table A.8).

Our results demonstrate that the relocation induced by China's cryptomining ban increased electricity consumption in the US, demonstrating that decarbonisation policies in developing countries can have spillovers on developed countries.

5.2.2 Impact on electricity generation

How did US power generation cater to this additional demand? As with consumption, we first show how US electricity generation changed relative to other countries, and then examine generation patterns in US mining vs non-mining states.

US vs other countries. We estimate an equation analogous to (6), comparing electricity generation in mining vs non-mining countries before vs after China's ban. Table A.9 shows that total generation increased in the US, but did not change in other mining countries (panel B, column 1). This mirrors our results on the relocation of cryptomining equipment, Bitcoin mining activity, and electricity consumption. The additional generation was mainly powered by fossil fuels, which accounted for two-thirds of the increase (columns 2 and 3).

Within US: Mining vs non-mining states. Comparing power generation in US mining vs non-mining states, before vs after China's ban, we find that monthly fossil generation in each mining state increased by 411 GWh, approximately 4% above the pre-ban mean (table A.10, panel A, column 2), with significant increases in all five mining states (panel C, column 2). By contrast, non-fossil generation does not show a consistent pattern, with increases in some mining states and decreases in others (column 3). These results are robust to controlling for COVID-19, night light intensity, the 2021 Texas freeze, or classifying California as a non-mining state (table A.11).

Taken together, our results suggest that the marginal electricity demand from cryptomining was mainly met by fossil-fuel generators. This finding for America's five mining states is consistent with the pattern we found across China's four mining provinces, including those with significant renewable capacity. Recall that when China banned cryptomining, it was coal generation in Inner Mongolia and Xinjiang that reduced most significantly (table 2). Our results are consistent with those of detailed study of a vertically integrated cryptomining facility in Pennsylvania, which documents that the plant burned more coal when mining incentives increased (Papp et al., 2023). This pattern could reflect cryptomining's demand for dispatchable power around the clock, which is usually supplied by fossil-fuel plants. Alternatively, by consuming renewable power, cryptominers may crowd out other users who then rely on fossil generation.

5.2.3 Response of US fossil-fuel power plants

We directly test the hypothesis that old, inefficient fossil-fuel plants expanded production to meet the demand from cryptominers, as noted by the press (Brian and Caitlin, 2021). Analysing the daily operations of over 1,000 fossil-fuel power plants, we estimate a triple difference regression, comparing generation by (i) old vs new power plants, (ii) in mining vs non-mining states, (iii) before vs after China's ban:

$$\begin{aligned} Y_{ijt} = &\beta_1 MiningState_i \times OlderPlant_j \times PostBan_t + \beta_2 OlderPlant_j \times PostBan_t + \\ &\beta_3 MiningState_i \times PostBan_t + \alpha_i + \alpha_j + \alpha_t + \epsilon_{imt} \end{aligned} \tag{7}$$

where Y_{ijt} is monthly electricity generation (or operating hours) of plant j in state i in month t. We include plant fixed effects and month-of-sample fixed effects, thus leveraging within-plant variation, and include state-by-month-of-year fixed effects to control for state-wise seasonal determinants of energy use and state-specific time trends. Older power plants are those above the median age, which is 18 years in our sample.

Table 6, confirms that the additional generation in mining states was predominantly from older plants (column 1). In non-mining states, generation from these older plants is sharply declining (row 2), suggesting that they are being phased out. Column 2 documents striking changes in coal-fired plants. New coal plants in mining states did not generate more power after the ban (row 3). However, old coal plants, which are being phased out in non-mining states (row 2), increased generation in mining states by $53 - 11 = 42$ GWh, about 10% of pre-ban levels (rows 1 and 3). These older plants tend to be less energy efficient and emit more CO_2 (figure A.13). By contrast, neither old nor new gas plants increased generation after the ban (column 3).

Panel B examines plant operating hours. After China's ban, old coal plants in mining states operated 1.8 more hours per day, a 13% increase, while gas and new coal plants did not change operating hours. These findings are robust to several checks, such as restricting attention to plant-months with positive generation, considering California a non-mining state, or clustering at the state rather than plant level (table A.12).

Our results are consistent with marginal electricity demand from cryptomining giving old, energy-inefficient, carbon-intensive coal plants in US mining states a new lease of life. The findings add fuel to the argument that cryptomining—a new data-intensive industry—is often powered by carbon-intensive energy sources.

5.3 Net global impacts of China's cryptomining ban

China's ban reduced domestic electricity consumption and fossil generation, but triggered a global migration of dirty physical capital that raised electricity consumption and fossil generation in the US. To assess the ban's net effects, we combine electricity data for 48 US states and 31 Chinese provinces to estimate the regression:

$$\begin{aligned} Y_{it} = &\beta_1 MiningLocation_i \times PostBan_t + \beta_2 China_i \times PostBan_t \\ &+ \beta_3 MiningLocation_i \times China_i \times PostBan_t + X_{it}^{'}\Gamma + \alpha_i + \alpha_t + \epsilon_{it} \end{aligned} \tag{8}$$

where Y_{it} denotes electricity consumption or generation for subnational unit i in month t. $MiningLocation_i$ is a dummy for cryptomining locations in both countries, i.e., the four Chinese provinces and five US states with major cryptomining operations prior to the ban. $PostBan_t$ takes value 1 from May 2021 onwards, $China_i$ is a dummy for Chinese provinces, and controls and standard errors are as in equation (1). Coefficient β_1 captures the ban's impact on US mining states, β_2 captures effects on non-mining Chinese provinces, and β_3 captures the differential effect on Chinese mining provinces. Our previous results suggest that we should expect $\beta_1 > 0$ and $\beta_3 < 0$.

We find that monthly electricity consumption fell by 1,692 GWh in each Chinese mining province and increased by 419 GWh in each US mining state (table A.13, column 1). Across the nine major mining locations, the ban caused a net 4,675 GWh decrease in monthly electricity consumption, about 0.5% of the US and China's combined energy use. The South-North displacement of mining activity diluted the impact of China's ban by 31%.[31]

Columns 2-3 show the ban's net effect on monthly electricity generation. While total generation does not significantly change, fossil generation fell by 1,421 GWh in each Chinese mining province and increased by 426 GWh in each US mining state—pointing to fossil fuels as the marginal generation source in both countries.[32] The ban's net effect was to reduce monthly fossil generation by 3,554 GWh, about 0.3% of the US-China combined level. The industry's relocation diluted the ban's impact on fossil generation by 37%.

Our electricity data runs till July 2023, about 2 years post-ban, allowing us to identify short- and medium-run impacts. Overall, our estimates suggest that China's ban decreased global electricity consumption and fossil generation, as Chinese declines outweighed US increases during this period. Even over this time horizon, miners' responses significantly attenuated the ban's global impact.

6 The impact of Ethereum's transition to Proof-of-Stake

Banning carbon-intensive industries will often not be economically prudent or politically feasible. In such contexts, an alternative decarbonisation strategy is to encourage firms to adopt cleaner production technologies. How effective these efforts are depends not just on the adopters of low-carbon processes, but also on whether dirty production

[31] The net effect is -1692×4 Chinese mining provinces + 419×5 US mining states = -4,675 GWh. We compute the dilution effect as $(419 \times 5)/(1692 \times 4) = 31\%$.

[32] The null effect on total generation may reflect some inter-province transmission to non-mining provinces, which we were able to observe directly in China.

factors are redeployed to alternative uses. Cryptomining again offers a valuable natural experiment to study this—a major coin's transition from the energy-intensive PoW consensus mechanism to the much greener PoS.

6.1 Empirical strategy: Regression Discontinuity in Time

As noted in section 2.3, Ethereum merged its Beacon chain and main network at exactly 2:45 am EST on 15 September 2022. That moment marked the world's second-largest cryptocurrency's complete transition from PoW to PoS, with mining intensity as proxied by its hashrate plummeting to zero just after the transition (figure A.1).

We evaluate the impact of Ethereum's transition using 2021-2023 hourly US electricity consumption and a Regression Discontinuity in Time (RDiT), following Hausman and Rapson (2018). First, we regress total hourly electricity consumption Y on weather controls and time fixed effects X. In the second stage, we regress first-stage residuals $\tilde{Y}$ on the running variable $Days\,to\,Transition_t$ and PoS_{th}, a dummy for whether date-hour th is after the Ethereum transition cutoff:

$$Y_{th} = X_{th}^{'}\Gamma + \xi_{th} \tag{9}$$

$$\tilde{Y_{th}} = \beta_1 PoS_{th} + \beta_2 Days\,to\,Transition_t + \beta_3 PoS_{th} \times Days\,to\,Transition_t + \varepsilon_{th} \tag{10}$$

Coefficient β_1 is the discontinuous change in electricity consumption at the moment when Ethereum transitions from PoW to PoS. First-stage controls include (i) temperature, precipitation and its square, dew point depression, and wind speed;[33] (ii) month-of-sample, year-by-day-of-week, federal holiday, and day-of-week-by-hour-of-day fixed effects. Following standard RD practice, we allow the running variable to have different slopes before and after the transition. Our baseline specification uses a 30-day bandwidth, but results are robust to alternative bandwidths.[34] Standard errors are bootstrapped at the date level with 500 replications (Hausman and Rapson, 2018).

[33] Weather controls are constructed by averaging hourly readings across all monitors within a state, and then taking the population-weighted average across state-hour readings. Temerature bins are 5°C wide.

[34] The data-driven optimal bandwidth proposed by Calonico et al. (2014) is not applicable in the RDiT setting because the running variable—time—is uniformly distributed around the cutoff.

6.2 Direct effects of Ethereum's transition on electricity use

US electricity consumption declined immediately upon Ethereum's transition to PoS (figure 3), with hourly consumption dropping by 16.6 GWh, a 3.2% reduction relative to the pre-transition mean (table 7, panel A, column 1). As we progressively increase the bandwidth from 30 to 365 days, the RD coefficient attenuates but remains negative and statistically significant. Taking the most conservative estimate, Ethereum's transition reduced hourly electricity consumption by 6.8 GWh, or 1.4% of the pre-transition mean. Our results are robust to several tests, such as excluding weather controls, controlling for 24-hour weather lags, or estimating "donut hole" RD regressions which omit observations right around the cutoff (table A.14).

Figures A.14 and A.15 report RD estimates separately by each state and balancing authority. Consistent with what we would expect, nearly all locations see a negative or null effect, and the decline is larger in states and balancing authority regions with more Ethereum nodes (table 7, panels B and C), our proxy for pre-transition Ethereum mining activity.[35]

These geographic patterns are difficult to reconcile with coincident shocks unrelated to mining, and confirm that Ethereum's adoption of a cleaner consensus mechanism reduced aggregate US electricity consumption

6.3 How cryptominers responded to Ethereum's transition

The RDiT estimates capture the instantaneous impact on electricity consumption of Ethereum "banning" the dirty production technology. However, as we learned from China's mining ban, owners of dirty capital are likely to respond rather than mothball their equipment. To test this, we examine mining activity for other PoW cryptocurrencies. Recall that PoW cryptocurrencies are typically mined using two types of hardware: ASICs, which specialise at a single task (e.g., Bitcoin's SHA-256 algorithm), and the more flexible multi-purpose GPUs, which are used for gaming, high-performance computing, and mining various cryptocurrency algorithms.

Ethereum was primarily mined using GPUs, because its Ethash algorithm was de-

[35] We do not have access to data on Ethereum mining locations. While Bitcoin can only be profitably mined at industrial scale, Ethereum is minable at smaller scales using standard GPUs. We scraped the IP addresses of all Ethereum nodes over the two weeks prior to the transition, and use this as a proxy for where Ethereum mining took place. This is an imperfect proxy, since Ethereum can be mined far from validator nodes.

signed to be ASIC-resistant.[36] Thus, after the transition, Ethereum miners could potentially redeploy their hardware to mine other GPU-minable cryptocurrencies—such as Ergo, Ethereum Classic and Ravencoin—but not ASIC-only coins like Bitcoin. We test for such substitution by comparing daily hashrates for these alternative cryptocurrencies just before vs after Ethereum's transition, applying the same RDiT estimator described in section 6.1.

Figure 4 shows that hashrates for GPU-minable cryptocurrencies spiked just after the transition. Ravencoin, Ergo, and Ethereum Classic experienced hashrate increases of 0.3-0.55 standard deviation—among the largest daily gains in their histories (figure A.16). By contrast, we see no change in Bitcoin mining activity, since it is exclusively ASIC-mined (figures 4 and A.16). These results suggest that some miners responded to Ethereum's transition by redeploying their hardware toward other cryptocurrencies that could be mined with the same equipment.

In total, hashrates for major, hardware-compatible substitute cryptocurrencies jumped by 245 TH/s just after Ethereum's transition.[37] Ethereum's pre-transition hashrate was about 830 TH/s (figure A.1), implying that cross-platform leakage offset roughly 30% of Ethereum's efforts almost immediately. This estimate likely represents a lower bound, as some hardware redeployment (e.g., use of second-hand GPUs in other industries) would likely take longer to materialise.

Our findings demonstrate a second way that firm responses can undermine decarbonisation policies—by redeploying production factors to other carbon-intensive economic activities. Prior work has documented pollution displacement (Davis, 2008; Aiello et al., 2023; Tanaka et al., 2022; Copeland et al., 2022), but there is comparatively little evidence on redeployment of carbon-intensive factors as a form of leakage.

[36]The Ethash algorithm was designed to be memory-hard, meaning that it required a lot of random-access memory to solve mining puzzles and precluded the efficient use of ASICs. By contrast, GPUs are good at memory-intensive tasks, making them ideal for Ethereum mining. Ethash was likely built to be ASIC-resistant to avoid the risk of centralising mining power in a few large miners.

[37]RD estimates are that hashrates increased by 140 TH/s for Ethereum Classic, 15 TH/s for Ravencoin, 30 TH/s for Ergo, 35 TH/s for Litecoin, and 25 TH/s for Dogecoin. A caveat is that the hash algorithms of different cryptocurrencies may vary in difficulty, so comparing hashrates across coins is not straightforward. The dilution ratio we report should be regarded as a rough approximation.

7 Discussion & Conclusion

7.1 External validity: Relevance for computation-heavy industries

Both China's ban and Ethereum's transition reduced the cryptocurrency industry's carbon emissions, but both policies were undermined by miners' responses to relocate and redeploy their equipment. How applicable are these findings to other emerging computation-heavy industries, such as AI?

Cryptomining and AI are distinct industries, but share several features that influence their carbon footprints. Both rely on energy-intensive computation—to solve PoW algorithms in cryptomining or to train predictive and large language models in AI. Both industries tend to cluster in regions with cheap, reliable electricity. Both require continuous, round-the-clock electricity, which is typically met at the margin by dispatchable power sources like fossil-fuel plants that can ramp up output on demand (Joskow, 2011).

Yet important differences remain. Cryptomining farms, facing regulatory uncertainty, often adopt modular, containerised setups that can be quickly relocated (Stoll et al., 2023). By contrast, AI data centres typically invest more in fixed infrastructure such as advanced cooling systems and fibre-optic connectivity, making them less footloose in the short term, though still more mobile than traditional heavy industries. Nevertheless, AI-related emissions are likely to be highly footloose, since cloud routing allows firms to reallocate AI workloads seamlessly across different facilities worldwide (Dodge et al., 2022).

Another difference between cryptomining and AI may lie in the versatility of their hardware. Most cryptominers, especially after Ethereum's transition, use specialised ASICs that efficiently solve specific PoW algorithms but are less useful for other purposes, leaving little scope for redeployment (Capponi et al., 2023). By contrast, AI data centres mainly work with multi-purpose GPUs, which are used to train LLMs models, but can also be employed for media rendering, real-time analytics, or other applications. In response to targeted decarbonisation policies, these other computation-heavy industries may have less scope to relocate but potentially greater ability to redeploy production factors across uses.

In sum, AI hardware may generally be more redeployable than cryptomining hardware, complicating efforts to regulate emissions absent a cleaner electricity grid.

7.2 Conclusion

This paper evaluated two major policies to decarbonise cryptomining, an energy-intensive sector with important similarities to other emerging, computation-heavy industries. Both policies reduced electricity demand and embedded carbon emissions in the activities they targeted, but their effects were significantly dampened by miners' nimble responses. The first policy, a national ban in China, the industry's largest market, triggered a rare South-to-North relocation that increased electricity demand and fossil-fuel generation in the US. The second, a change in production technology by Ethereum, the industry's second-biggest platform, saw asset owners redeploy their sunk multi-purpose GPU capital to mine substitute cryptocurrencies. In both cases, dedicated computational equipment migrated to regions and uses less constrained by the original decarbonisation policy.

These findings highlight that even ambitious policies which reduce local emissions may have much smaller global effects when workloads are mobile and hardware can be redeployed. Effective decarbonisation will therefore require coordinated approaches that account for both geographic relocation and cross-use leakage. For example, adopters of cleaner digital technologies, such as PoS cryptominers and reduced-computation AI model developers, could push for emissions disclosure and pricing across the digital goods sector, much like the International Maritime Organization's consideration of a global carbon tax on shipping.

Our results indicate that cryptomining was powered at the margin by fossil fuels, even in Chinese provinces and US states with substantial renewable capacity. This finding cautions against claims that energy-hungry digital goods are environmentally benign when they operate in renewable-rich regions, and highlights the importance of pricing electricity at its social marginal cost.

Several questions remain for future research. One priority is to test whether data centres and other computation-heavy industries are similarly supplied by fossil generators at the margin—and examine whether grid-scale battery storage can alter this relationship. Another is to study the local air quality and public health impacts of cryptomining restrictions, given the documented effects of coal generation (Deschênes et al., 2017). As AI adoption accelerates alongside the climate transition, understanding how to decarbonise computation-heavy industries will become increasingly important.

References

Aiello, D., Baker, S. R., Balyuk, T., Di Maggio, M., Johnson, M. J., and Kotter, J. D. (2023). The Effects of Cryptocurrency Wealth on Household Consumption and Investment. NBER Working Paper 31445.

Alvarez, F., Argente, D., and Van Patten, D. (2022). Are Cryptocurrencies Currencies? Bitcoin as Legal Tender in El Salvador. NBER Working Paper 29968.

Andersson, J. J. (2019). Carbon taxes and co2 emissions: Sweden as a case study. *American Economic Journal: Economic Policy*, 11(4):1–30.

Arkhangelsky, D., Athey, S., Hirshberg, D. A., Imbens, G. W., and Wager, S. (2021). Synthetic Difference-in-Differences. *American Economic Review*, 111(12):4088–4118.

Asif, R. and Hassan, S. R. (2023). Shaping the Future of Ethereum: Exploring Energy Consumption in Proof-of-Work and Proof-of-Stake Consensus. *Frontiers in Blockchain*, 6:1151724.

Bateman, T. (2022). EU Regulator Calls for a Ban on Proof of Work Bitcoin Mining to Save Renewable Energy. www.euronews.com/next/2022/01/19/eu-regulator-calls-for-a-ban-on-proof-of-work-bitcoin-mining-to-save-renewable-energy. (accessed January 9, 2024).

Benetton, M. and Compiani, G. (2024). Investors' Beliefs and Cryptocurrency Prices. *Review of Asset Pricing Studies*, 14(2):197–236.

Benetton, M., Compiani, G., and Morse, A. (2023). When Cryptomining Comes to Town: High Electricity-use Spillovers to the Local Economy. NBER Working Paper 31312.

Biais, B., Capponi, A., Cong, L. W., Gaur, V., and Giesecke, K. (2023). Advances in Blockchain and Crypto Economics. *Management Science*, 69(11):6417–6426.

Bitmain (2022). https://support.bitmain.com/hc/en-us/articles/223761507-HS-Codes-for-Different-Regions. (accessed March 31, 2024).

Borenstein, S. (2012). The Private and Public Economics of Renewable Electricity Generation. *Journal of Economic Perspectives*, 26(1):67–92.

Borrero, M., Gowrisankaran, G., and Langer, A. (2023). Ramping Costs and Coal Generator Exit. Technical report, Working Paper.

Borri, N. and Shakhnov, K. (2020). Regulation Spillovers across Cryptocurrency Markets. *Finance Research Letters*, 36:101333.

Braiins (2020). Data Privacy and Security for Bitcoin Miners. https://braiins.com/blog/data-privacy-and-security-for-bitcoin-miners.

Brian, S. and Caitlin, O. (2021). Bitcoin Miners Are Giving New Life to Old Fossil-Fuel Power Plants. www.wsj.com/articles/bitcoin-miners-are-giving-new-life-to-old-fossil-fuel-power-plants-11621594803. (accessed June 21, 2024).

Budish, E. (2024). Trust at Scale: The Economic Limits of Cryptocurrencies and Blockchains. *The Quarterly Journal of Economics*, 140(1):1–62.

Bushnell, J. (2024). Is there a "Duty to Serve"' Hyperscale Loads? https://energyathaas.wordpress.com/2024/12/02/is-there-a-duty-to-serve-hyperscale-loads/. (accessed January 17, 2025).

Butters, R. A., Dorsey, J., and Gowrisankaran, G. (2025). Soaking up the sun: Battery investment, renewable energy, and market equilibrium. *Econometrica*, 93(3):891–927.

Calel, R., Colmer, J., Dechezleprêtre, A., and Glachant, M. (2025). Do Carbon Offsets Offset Carbon? *American Economic Journal: Applied Economics*, 17(1):1–40.

Calonico, S., Cattaneo, M. D., and Titiunik, R. (2014). Robust Nonparametric Confidence Intervals for Regression-Discontinuity Designs. *Econometrica*, 82(6).

Capponi, A., Olafsson, S., and Alsabah, H. (2023). Proof-of-Work Cryptocurrencies: Does Mining Technology Undermine Decentralization? *Management Science*, 69(11):6455–6481.

Chamanara, S., Ghaffarizadeh, S. A., and Madani, K. (2023). The Environmental Footprint of Bitcoin Mining Across the Globe: Call for Urgent Action. *Earth's Future*, 11(10):e2023EF003871.

Chen, C. and Liu, L. (2022). How Effective is China's Cryptocurrency Trading Ban? *Finance Research Letters*, 46:102429.

Clarke, D., Muñoz, P., and Rosales, M. (2023). Synthetic Difference-In-Differences Estimation. SSRN 4346540.

Clausing, K. A., Colmer, J. M., Hsiao, A., and Wolfram, C. (2025). The global effects of carbon border adjustment mechanisms. Technical report, National Bureau of Economic Research.

CoinMarketCap (2024). https://coinmarketcap.com/. (accessed January 28, 2024).

Colmer, J., Martin, R., Muûls, M., and Wagner, U. J. (2025). Does Pricing Carbon Mitigate Climate Change? Firm-Level Evidence from the European Union Emissions Trading System. *The Review of Economic Studies*, 92(3):1625–1660.

Cong, L. W., Ghosh, P., Li, J., and Ruan, Q. (2024). Inflation Expectation and Cryptocurrency Investment. NBER Working Paper 32945.

Cong, L. W., Li, X., Tang, K., and Yang, Y. (2023). Crypto Wash Trading. *Management Science*, 69(11):6427–6454.

Copeland, B. R., Shapiro, J. S., and Taylor, M. S. (2022). Globalization and the Environment. In *Handbook of International Economics*, volume 5, pages 61–146. Elsevier.

Davis, L. W. (2008). The Effect of Driving Restrictions on Air Quality in Mexico City. *Journal of Political Economy*, 116(1):38–81.

De Vries, A. (2018). Bitcoin's Growing Energy Problem. *Joule*, 2(5):801–805.

De Vries, A., Gallersdörfer, U., Klaaßen, L., and Stoll, C. (2022). Revisiting Bitcoin's Carbon Footprint. *Joule*, 6(3):498–502.

Deschênes, O., Greenstone, M., and Shapiro, J. S. (2017). Defensive Investments and the Demand for Air Quality: Evidence from the NOx Budget Program. *American Economic Review*, 107(10):2958–89.

Dodge, J., Prewitt, T., Tachet des Combes, R., Odmark, E., Schwartz, R., Strubell, E., Luccioni, A. S., Smith, N. A., DeCario, N., and Buchanan, W. (2022). Measuring the carbon intensity of ai in cloud instances. In *Proceedings of the 2022 ACM conference on fairness, accountability, and transparency*, pages 1877–1894.

Dugoua, E. and Moscona, J. (2025). The Economics of Climate Innovation: Technology, Climate Policy, and the Clean Energy Transition. Technical report, National Bureau of Economic Research.

Eskeland, G. S. and Harrison, A. E. (2003). Moving to Greener Pastures? Multinationals and the Pollution Haven Hypothesis. *Journal of Development Economics*, 70(1):1–23.

Farrokhi, F. and Lashkaripour, A. (2025). Can trade policy mitigate climate change? *Econometrica*, 93(5):1561–1599.

Feng, C. (2021). BTCChina, Country's First Bitcoin Exchange, Gives Up Cryptocurrency Amid Regulatory Crackdown. https://www.scmp.com/tech/policy/article/3138618/btcchina-countrys-first-bitcoin-exchange-gives-cryptocurrency-amid. (accessed July 19, 2024).

Foteinis, S. (2018). Bitcoin's Alarming Carbon Footprint. *Nature*, 554(7690):169–170.

Gallersdörfer, U., Klaaßen, L., and Stoll, C. (2020). Energy Consumption of Cryptocurrencies Beyond Bitcoin. *Joule*, 4(9):1843–1846.

Gibson, M. (2019). Regulation-Induced Pollution Substitution. *The Review of Economics and Statistics*, 101(5):827–840.

Goodkind, A. L., Jones, B. A., and Berrens, R. P. (2020). Cryptodamages: Monetary Value Estimates of the Air Pollution and Human Health Impacts of Cryptocurrency Mining. *Energy Research & Social Science*, 59:101281.

Gowrisankaran, G., Reynolds, S. S., and Samano, M. (2016). Intermittency and the Value of Renewable Energy. *Journal of Political Economy*, 124(4):1187–1234.

Graff Zivin, J. S., Kotchen, M. J., and Mansur, E. T. (2014). Spatial and Temporal Heterogeneity of Marginal Emissions: Implications for Electric Cars and Other Electricity-Shifting Policies. *Journal of Economic Behavior & Organization*, 107:248–268.

Greenstone, M., Pande, R., Ryan, N., and Sudarshan, A. (2025). Can Pollution Markets Work in Developing Countries? Experimental Evidence from India. *The Quarterly Journal of Economics*, 140(2):1003–1060.

Halaburda, H., Haeringer, G., Gans, J., and Gandal, N. (2022). The Microeconomics of Cryptocurrencies. *Journal of Economic Literature*, 60(3):971–1013.

Halaburda, H. and Yermack, D. (2023). Bitcoin Mining Meets Wall Street: A Study of Publicly Traded Crypto Mining Companies. NBER Working Paper 30923.

Hale, T., Angrist, N., Goldszmidt, R., Kira, B., Petherick, A., Phillips, T., Webster, S., Cameron-Blake, E., Hallas, L., Majumdar, S., and Tatlow, H. (2021). A Global Panel Database of Pandemic Policies (Oxford COVID-19 Government Response Tracker). *Nature Human Behaviour*, 5(4):529–538.

Hanna, R. (2010). US Environmental Regulation and FDI: Evidence from a Panel of US-Based Multinational Firms. *American Economic Journal: Applied Economics*, 2(3):158–189.

Hansen-Lewis, J. and Marcus, M. (2025). Uncharted Waters: Effects of Maritime Emission Regulation. *American Economic Journal: Economic Policy*, 17(1):37–69.

Hausman, C. and Rapson, D. S. (2018). Regression Discontinuity in Time: Considerations for Empirical Applications. *Annual Review of Resource Economics*, 10:533–552.

He, G., Wang, S., and Zhang, B. (2020). Watering Down Environmental Regulation in China. *The Quarterly Journal of Economics*, 135(4):2135–2185.

Hong, H. and Chen, K. (2026). When the Fire Ends: Straw Burning, Regulation, and Pollution Substitution. *Journal of Development Economics*, 181:103727.

Hsiao, A. (2026). Coordination and commitment in international climate action: evidence from palm oil. *Econometrica*, 94(1):1–33.

Iyoha, E., Malesky, E., Wen, J., Wu, S.-J., and Feng, B. (2024). Exports in Disguise?: Trade Rerouting during the US-China Trade War. *Unpublished manuscript*.

Jermann, U. and Xiang, H. (2025). Tokenomics: Optimal Monetary and Fee Policies. *Journal of Monetary Economics*, page 103808.

John, K., O'Hara, M., and Saleh, F. (2022). Bitcoin and Beyond. *Annual Review of Financial Economics*, 14(1):95–115.

Jones, B. A., Goodkind, A. L., and Berrens, R. P. (2022). Economic Estimation of Bitcoin Mining's Climate Damages Demonstrates Closer Resemblance to Digital Crude than Digital Gold. *Scientific Reports*, 12(1):14512.

Joskow, P. L. (2011). Comparing the Costs of Intermittent and Dispatchable Electricity Generating Technologies. *American Economic Review*, 101(3):238–241.

Kaiser, B., Jurado, M., and Ledger, A. (2018). The Looming Threat of China: An Analysis of Chinese Influence on Bitcoin. arXiv:1810.02466.

Klenow, P. J., Pastén, E., and Ruane, C. (2024). Carbon taxes and misallocation in chile. Technical report, Technical Report, Mimeo, Stanford.

Kranz, S. (2022). Synthetic Difference-in-Differences with Time-Varying Covariates. Technical report, Available online at: https://github. com/skranz/xsynthdid.

Krause, M. J. and Tolaymat, T. (2018). Quantification of Energy and Carbon Costs for Mining Cryptocurrencies. *Nature Sustainability*, 1(11):711–718.

Levinson, A. (2023). Are Developed Countries Outsourcing Pollution? *Journal of Economic Perspectives*, 37(3):87–110.

Lin, M.-B., Găman, S., Wang, R., and Pele, D. T. (2025). Market Responses to Ethereum Development Milestones: An Event Study Approach. SSRN 5176758.

Liu, S., Yang, Q., Cai, H., Yan, M., Zhang, M., Wu, D., and Xie, M. (2019). Market Reform of Yunnan Electricity in Southwestern China: Practice, Challenges and Implications. *Renewable and Sustainable Energy Reviews*, 113:109265.

Liu, Y. and Tsyvinski, A. (2021). Risks and Returns of Cryptocurrency. *Review of Financial Studies*, 34(6):2689–2727.

Lu, W., Yuan, Y., and Zhang, F. (2025). A Story of Fire and Water: Cryptocurrency, Nomad Miners, and the Environment. SSRN 5348921.

Makarov, I. and Schoar, A. (2020). Trading and Arbitrage in Cryptocurrency Markets. *Journal of Financial Economics*, 135(2):293–319.

Makarov, I. and Schoar, A. (2022). Cryptocurrencies and Decentralized Finance (DeFi). *Brookings Papers on Economic Activity*, 2022(1):141–215.

Ortiz-Villavicencio, M. and Sant'Anna, P. H. (2025). Better Understanding Triple Differences Estimators. arXiv:2505.09942.

Pan, D. (2021). Why China's Ban on Crypto Mining Is More Serious Than Before. www.coindesk.com/policy/2021/07/09/why-chinas-ban-on-crypto-mining-is-more-serious-than-before/. (accessed January 9, 2024).

Papp, A., Almond, D., and Zhang, S. (2023). Bitcoin and Carbon Dioxide Emissions: Evidence from Daily Production Decisions. *Journal of Public Economics*, 227:105003.

Sharma, R. (2023). China's History With Cryptocurrency. www.investopedia.com/news/price-cryptocurrencies-totally-dependent-china/. (accessed January 9, 2024).

Sockin, M. and Xiong, W. (2023). A Model of Cryptocurrencies. *Management Science*, 69(11):6684–6707.

Stoll, C., Klaaßen, L., and Gallersdörfer, U. (2019). The Carbon Footprint of Bitcoin. *Joule*, 3(7):1647–1661.

Stoll, C., Klaaßen, L., Gallersdörfer, U., and Neumüller, A. (2023). *Climate Impacts of Bitcoin Mining in the US*. MIT Center for Energy and Environmental Policy Research.

Tanaka, S., Teshima, K., and Verhoogen, E. (2022). North-South Displacement Effects of Environmental Regulation: The Case of Battery Recycling. *American Economic Review: Insights*, 4(3):271–288.

US CBP (2018). U.S. Customs and Border Protection https://rulings.cbp.gov/ruling/N297495. (accessed March 31, 2024).

US EIA (2023). Frequently Asked Questions: Crude Oil, Gasoline, Heating Oil, Diesel, Propane, and Other Liquids—Including Biofuels and Natural Gas Liquids. U.S. Energy Information Administration, https://www.eia.gov/tools/faqs/faq.php?id=74&t=11. (accessed August 26, 2025).

Zou, E. Y. (2021). Unwatched Pollution: The Effect of Intermittent Monitoring on Air Quality. *American Economic Review*, 111(7):2101–2126.

Tables

Table 1: Domestic Impacts of China's Mining Ban—Electricity Consumption

Dependent variable is	DiD		SDiD
Electricity consumption (GWh)	(1)	(2)	(3)
Mining Province × Post Ban	-1169.9*		-1039.2**
	(669.0)		(524.0)
Inner Mongolia × Post Ban		-2867.4***	
		(153.8)	
Xinjiang × Post Ban		-443.7*	
		(225.4)	
Sichuan × Post Ban		354.1	
		(230.8)	
Yunnan × Post Ban		-1737.6***	
		(213.5)	
Dependent variable mean prior to ban for Mining Province	23,234.6	23,234.6	23,234.6
Number of observations	2077	2077	2077

Notes: This table presents estimates from our baseline DiD specification, i.e., estimates of β from equation (1). The dependent variable is total electricity consumption (GWh) for province i in month t for 31 provinces from January 2018 to July 2023. Dummy variable *Mining Province* indicates major cryptomining provinces before the ban, and is 1 for Inner Mongolia, Xinjiang, Sichuan, and Yunnan. Dummy *Post Ban* denotes months from May 2021 onwards. Columns 1-2 present OLS estimates and column 3 presents synthetic DiD estimates. All regressions include province-by-month-of-year and month-of-sample fixed effects, province-specific time trends, and weather controls (5°C temperature bins, precipitation and its square, dew point depression, and wind speed). Standard errors are clustered by province in columns 1-2 and cluster-bootstrapped with 1000 replications in column 3. Significant at *10%, **5%, and ***1%. Results are discussed in section 4.2. Dynamic DiD graphs are presented in figure 1. Robustness results are in tables A.3 and A.4.

Table 2: Domestic Impacts of China's Mining Ban—Electricity Generation & Inter-Province Transmission

Dependent variable is:	Electricity generation (GWh)					Electricity exports (GWh)
		Renewable sources				
	Fossil	Hydro	Wind	Solar	Total	
	(1)	(2)	(3)	(4)	(5)	(6)
Panel A. DiD						
Mining Province × Post Ban	-953.3**	1131.4**	-70.2	-21.6	130.0	1679.0**
	(396.0)	(508.9)	(159.6)	(39.7)	(684.6)	(650.7)
Panel B. SDiD						
Mining Province × Post Ban	-933.0	530.6***	-50.9	-63.9*	-263.5	1685.5*
	(776.6)	(183.8)	(306.0)	(38.0)	(749.9)	(981.0)
Panel C. Response by province (DiD)						
Inner Mongolia × Post Ban	-1795.9***	2.0	427.9***	-90.9***	-1413.6***	1358.3***
	(224.7)	(78.1)	(49.0)	(16.5)	(213.5)	(165.1)
Xinjiang × Post Ban	-1014.0***	351.8***	-236.6***	94.6***	-762.0***	15.8
	(218.4)	(80.9)	(47.6)	(16.0)	(196.5)	(170.0)
Sichuan × Post Ban	-110.1	1853.5***	-188.2***	-52.1***	1539.6***	3369.5***
	(255.5)	(79.5)	(54.9)	(14.4)	(242.8)	(160.2)
Yunnan × Post Ban	-902.9***	2304.9***	-281.7***	-37.8**	1135.6***	1953.2***
	(243.9)	(74.4)	(45.2)	(14.5)	(221.8)	(180.6)
Dep. var. mean prior to ban for Mining Province	17,260.4	12,143.6	2817.5	545.4	32,766.9	11,705.4
Number of observations	2077	2077	2077	2077	2077	2010

Notes: This table presents standard and synthetic DiD estimates from our baseline specification, equation (1), as indicated in the panels. An observation is a province-month pair, and the sample covers 31 provinces from January 2018 to July 2023. The last column drops observations for Beijing as this province's 2023 data are missing and the SDiD estimator requires a balanced panel. The dependent variable is fossil-fuel generation in column 1; hydroelectric, wind, and solar generation in columns 2-4; total electricity generation across all energy sources in column 5; and inter-province electricity exports in column 6. As in table 1, *Mining Province* denotes the four major cryptomining provinces before the ban and *Post Ban* denotes months from May 2021 onwards; fixed effects and controls are also as in table 1. Standard errors are clustered by province in panels A and C and cluster-bootstrapped with 1000 replications in panel B. Significant at *10%, **5%, and ***1%. Results are discussed in section 4.3. Dynamic DiD graphs are presented in figures 1 (fossil generation), A.6 (renewable generation) and A.8 (total generation and exports). Robustness results are in tables A.3 and A.4.

Table 3: Global Spillovers of China's Mining Ban—Chinese Exports of Cryptomining Equipment

Dependent variable is	Average treatment effect on:	
Export value (million USD)	Six mining countries	US versus other mining countries
	(1)	(2)
Panel A. OLS DDD Estimator		
Mining Equipment × Mining Country	14.9***	
× Post Ban	(5.7)	
Mining Equipment × US × Post Ban		33.8***
		(9.9)
Mining Equipment × Other Mining Countries		11.1*
× Post Ban		(5.8)
Panel B. Doubly Robust DDD Estimator		
Mining Equipment × Mining Country	12.1*	
× Post Ban	(6.7)	
Mining Equipment × US × Post Ban		33.1***
		(9.8)
Mining Equipment × Other Mining Countries		7.9
× Post Ban		(6.0)
Dep.var. mean pre-ban for Mining Country	48.9	
Dep.var. mean pre-ban for US		230.6
Dep.var. mean pre-ban for non-US		12.5
Number of observations	50,050	50,050

Notes: This table shows triple-difference regression estimates based on equation (3). An observation is a destination country-HS8 product-month triple. The sample covers 52 destination countries and 18 HS8-digit products (all within Chinese industry 4042 and in the same HS4 group as cryptomining equipment) between January 2019 and July 2023. Small destination countries are grouped into a single "country"—rest of world. The dependent variable is Chinese exports (in USD million, base January 2019) of product j to country i in month t. *Mining Equipment* denotes cryptomining machines (HS8 code 84715040) and hashboards (HS8 code 84733090). *Mining Country* denotes major cryptomining countries before China's ban: the US, Malaysia, Kazakhstan, Canada, Russia, and Iran. *Other Mining Countries* refers to major cryptomining countries except the US. *Post Ban* denotes months from May 2021 onwards. All regressions include destination-by-HS8 product, destination-by-month, and HS8 product-by-month fixed effects. Panel A presents OLS estimates while panel B shows results from Ortiz-Villavicencio and Sant'Anna (2025)'s doubly robust estimator. Standard errors are clustered at the destination-by-HS8 product level. Significant at *10%, **5%, and ***1%. Results are discussed in section 5.1 and further presented in figures A.9 and A.10.

Table 4: Global Spillovers of China's Mining Ban—Imports of Cryptomining Equipment by US Mining States

Dependent variable is Import value (million USD)	All inputs (1)	Mining machines (2)	Hashboards (3)
Panel A. OLS DDD Estimator			
Mining Equipment × Mining State	46.4**	39.0**	55.0
× Post Ban	(23.1)	(16.1)	(42.4)
Panel B. Doubly-Robust DDD Estimator			
Mining Equipment × Mining State	34.5**	35.3*	36.8*
× Post Ban	(14.0)	(20.7)	(21.7)
Mean of import value from world prior to ban for Mining State of Mining Equipment	143.7	44.0	243.5
Number of importing states	48	48	48
Number of HS6 products	26	19	7
Number of observations	68,640	50,160	18,480

Notes: This table shows triple difference regression estimates based on equation (5). An observation is a state-HS6 product-month triple. The dependent variable is imports (in USD million, base January 2019) of product j by US state i in month t. *Mining Equipment* denotes cryptomining machines and hashboards in column 1, only cryptomining machines in column 2, and only hashboards in column 3. *Mining State* indicates major US cryptomining states before the ban, and is 1 for Texas, Georgia, New York, Kentucky, and California. *Post Ban* denotes months from May 2021 onwards. The sample covers the 48 US contiguous states between January 2019 and July 2023. Products in the estimation sample vary by column: column 1 includes cryptomining equipment (both cryptomining machines and hashboards) and 24 other HS6 products; column 2 restricts to cryptomining machines and 18 other HS6 products in NAICS industry 335999; and column 3 restricts to hashboards and 6 other HS6 products in NAICS industry 333242. All regressions include state-by-HS6 product, state-by-month, and HS6 product-by-month fixed effects. Standard errors are clustered at the state-by-HS6 product level. Panel A presents OLS estimates while panel B shows results from Ortiz-Villavicencio and Sant'Anna (2025)'s doubly robust estimator. Significant at *10%, **5%, and ***1%. Results are discussed in section 5.1 and further presented in figure A.10.

Table 5: Global Spillovers of China's Mining Ban—Impacts on US Electricity Consumption

Dependent variable is Electricity consumption (GWh)	All sectors (1)	Commercial/Industrial (2)	Residential (3)
Panel A. DiD			
Mining State × Post Ban	415.6***	514.9**	-103.1
	(141.0)	(195.6)	(63.9)
Panel B. SDiD			
Mining State × Post Ban	366.3***	462.3**	-107.9
	(134.9)	(226.4)	(154.9)
Panel C. Response by US state (DiD)			
Texas × Post Ban	794.9***	929.5***	-135.3***
	(29.3)	(27.0)	(8.5)
Georgia × Post Ban	172.0***	193.4***	-22.4*
	(29.7)	(26.3)	(12.2)
New York × Post Ban	233.5***	243.4***	-18.1*
	(32.6)	(28.1)	(9.7)
Kentucky × Post Ban	121.0***	91.8***	29.6**
	(30.8)	(26.6)	(11.2)
California × Post Ban	759.3***	1120.4***	-370.8***
	(33.3)	(28.2)	(18.3)
Dependent variable mean prior to ban for Mining State	17,103.1	10,688.2	6351.8
Number of observations	3216	3216	3216

Notes: This table presents results for DiD regressions akin to equation (1). Panels A and C contain standard DiD estimates while Panel B contains synthetic DiD estimates. An observation is a US state-month pair, and the sample covers the 48 contiguous US states from January 2018 to July 2023. The dependent variable is electricity consumption (GWh) across all sectors in column 1, in the commercial and industrial sectors only in column 2, and in the residential sector only in column 3. *Mining State* denotes major cryptomining states before China's ban, and is 1 for Texas, Georgia, New York, Kentucky, and California. *Post Ban* denotes months from May 2021 onwards. All regressions include state-by-month-of-year and month-of-sample fixed effects, state-specific time trends, and weather controls (as in table 1). Standard errors are clustered by state in panels A and C and cluster-bootstrapped with 1000 replications in panel B. Significant at *10%, **5%, and ***1%. Results are discussed in section 5.2 and further presented in figure A.12.

Table 6: Global Spillovers of China's Mining Ban—Impacts on US Fossil-fuel Electricity Generation

	All fossil-	Primary fuel type	
	fuel plants	Coal	Gas
	(1)	(2)	(3)
Panel A: Electricity generation (GWh)			
Mining State × Older Plant × Post Ban	11.72*	53.06**	-2.22
	(6.48)	(24.29)	(6.02)
Older Plant × Post Ban	-20.15***	-30.02**	-5.32*
	(3.78)	(12.82)	(3.09)
Mining State × Post Ban	-9.83*	-11.12	6.28
	(5.15)	(23.78)	(4.70)
Dependent variable mean prior to ban for plants in Mining State	137.80	424.68	107.09
Number of plants	1250	275	975
Number of observations	79,453	16,161	63,292
Panel B: Daily average operating hours			
Mining State × Older Plant × Post Ban	0.44	1.86**	-0.03
Post Ban	(0.30)	(0.92)	(0.31)
Older Plant × Post Ban	-0.58***	-0.72	-0.04
	(0.16)	(0.45)	(0.16)
Mining State × Post Ban	-0.25	-0.64	0.32
	(0.24)	(0.78)	(0.25)
Dependent variable mean prior to ban for plants in Mining State	8.24	14.70	7.55
Number of plants	1250	275	975
Number of observations	79,485	16,173	63,312

Notes: This table presents estimates from six DiD regressions based on equation (7). The dependent variable is either monthly electricity generation (panel A) or daily average operating hours (panel B) of power plant i in month t. An observation is a plant-month pair, and the time period of analysis is January 2018 to July 2023. The sample is trimmed to exclude outliers (top and bottom 0.5% of the distribution). *Mining State* is a dummy that takes value 1 for the five states with significant Bitcoin mining activity before China's ban (Texas, Georgia, New York, Kentucky, California). *Post Ban* denotes months from May 2021 onwards. *Older Plant* are those with above median age across all fossil plants (column 1) or coal plants (column 2) or natural gas plants (column 3). All regressions include plant, state-by-month-of-year, and month-of-sample fixed effects, state-specific time trends, and weather controls (as in table 1). Standard errors are clustered by plant. Significant at *10%, **5%, and ***1%. Results are discussed in section 5.2.3.

Table 7: Ethereum's Transition to Proof-of-Stake—Impacts on US Electricity Consumption

	Dependent variable: Hourly electricity consumption (GWh)					
Panel A. Nationwide series						
Bandwidth (days):	30 days	60 days	90 days	180 days	270 days	365 days
	(1)	(2)	(3)	(4)	(5)	(6)
Post Ethereum Transition	-16.6***	-14.6***	-13.7***	-12.0***	-8.7***	-6.8***
	(3.9)	(3.6)	(3.3)	(2.5)	(2.0)	(1.4)
Dep. var. mean pre-shift in the bandwidth	518.0	542.2	541.6	492.0	482.9	469.5
Number of observations	1439	2879	4319	8639	12,959	17,519
	Mean share of Ethereum node across regions or states (%)	Dependent variable mean 30 days prior to Ethereum Transition	Coefficient on Post Ethereum Transition (with a 30-day bandwidth)	Bootstrap standard error		
Panel B. Response by US balancing authority						
Top 1-10	8.15	30.42	-0.87***	(0.40)		
Top 11-20	1.15	10.23	-0.31**	(0.18)		
Top 21-30	0.51	8.09	-0.29***	(0.14)		
Top 31-40	0.10	1.41	-0.05**	(0.03)		
Other regions	0.03	1.54	-0.09***	(0.03)		
Panel C. Response by US state						
Top 1-10	8.31	27.11	-1.06***	(0.37)		
Top 11-20	1.16	10.72	-0.33**	(0.18)		
Top 21-30	0.38	8.40	-0.06	(0.16)		
Top 31-40	0.08	2.67	-0.04	(0.05)		
Other states	0.01	4.36	-0.08*	(0.09)		

Notes: This table presents estimates from our RDiT specification (section 6.1). The dependent variable is US hourly electricity consumption across all sectors (GWh). An observation is a date-hour pair and the sample covers the period 1 January 2021 to 31 December 2023. Panel A shows estimates for six different bandwidths. *Post Ethereum Transition* is a dummy for all date-hours after Ethereum's transition at 2:45am EST on 15 September 2022. Panels B and C present RDiT estimates for different US balancing authority or state subsamples. We divide balancing authorities and states by the number of Ethereum nodes, and stratify them by rank (top 1-10, top 11-20, etc). All regressions in panels B and C use a 30-day bandwidth. Regressions in all panels include month-of-sample, year-by-day-of-week, federal holiday, and day-of-week-by-hour-of-day fixed effects, as well as controls for temperature, precipitation and its square, dew point depression, and wind speed. Standard errors are bootstrapped at the date level with 500 replications. Significant at *10%, **5%, and ***1%. Results are discussed in section 6.2 and further presented in figures 3, A.14, and A.15.

Figures

Figure 1: Domestic Impacts of China's Mining Ban—Electricity Consumption & Fossil Generation

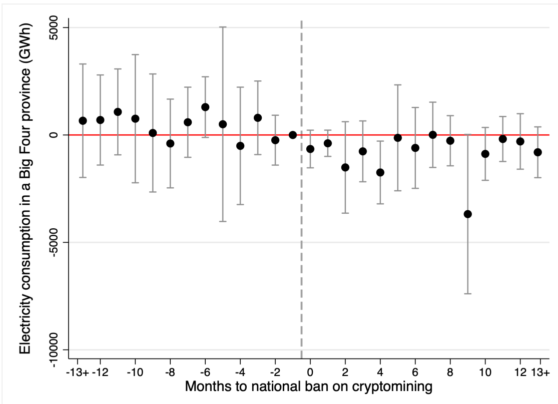

(**a**) DiD: Electricity consumption

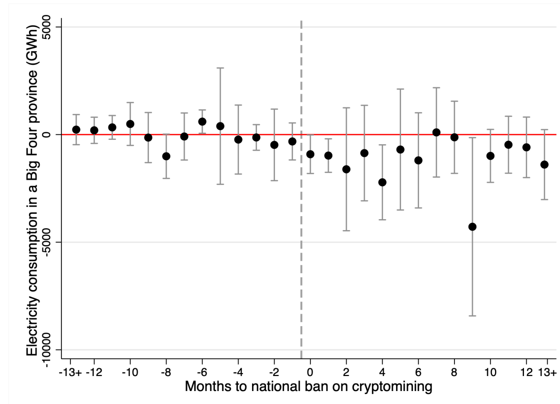

(**b**) SDiD: Electricity consumption

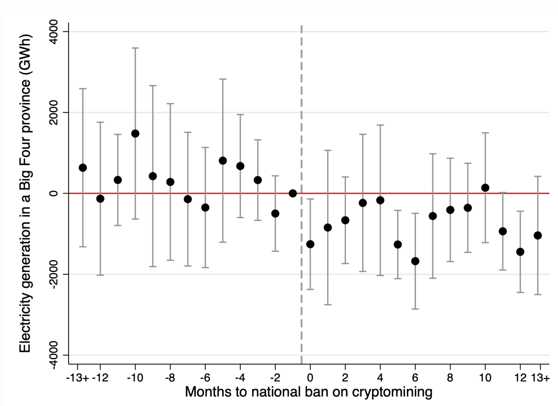

(**c**) DiD: Electricity generation, fossil

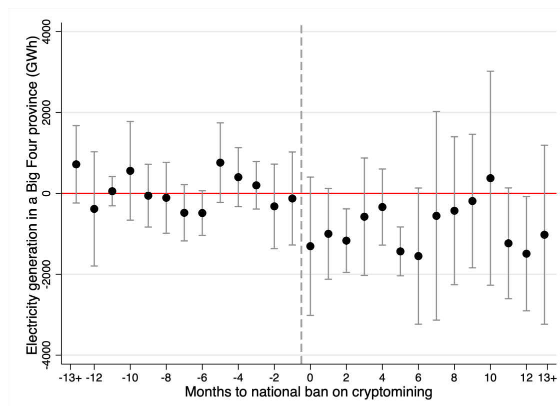

(**d**) SDiD: Electricity generation, fossil

Notes: These figures show dynamic DiD coefficients from estimating equation (2). We present the set of β_k, coefficients on the $MiningProvince_i$ dummy k months from China's ban. The dots denote point estimates and spikes 95% confidence intervals. The dependent variable is total electricity consumption in panels (a)-(b) and fossil-fuel generation in panels (c)-(d). Panels (a) and (c) present coefficients based on the DiD model whereas panels (b) and (d) present SDiD coefficients. All regressions include province-by-month-of-year and month-of-sample fixed effects, province-specific time trends, and weather controls. Tables 1 and 2 report regression estimates. Results on electricity consumption and generation are discussed in sections 4.2 and 4.3, respectively.

Figure 2: Global Spillovers of China's Mining Ban—Impact on Bitcoin Mining Activity in Other Mining Countries

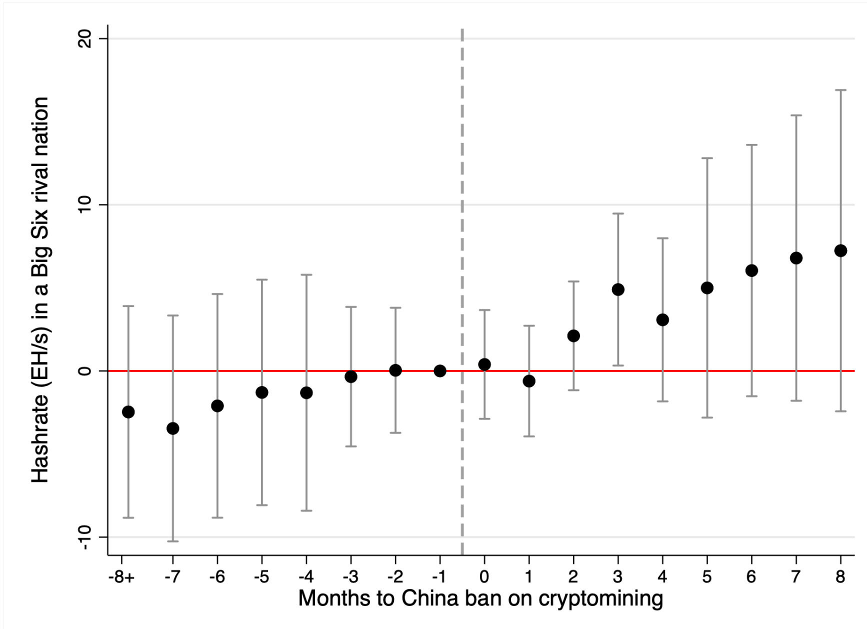

(**a**) DiD: Bitcoin hashrate

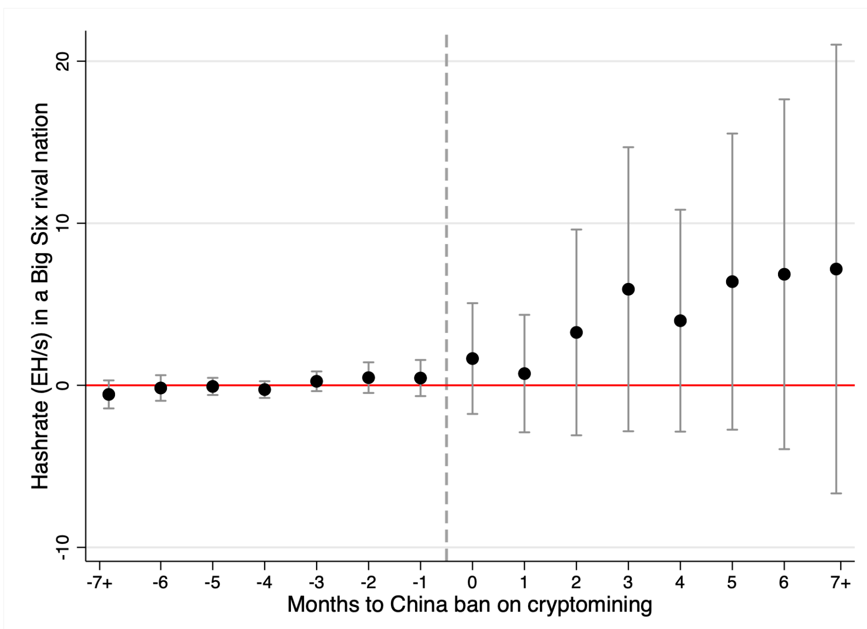

(**b**) SDiD: Bitcoin hashrate

Notes: These figures show dynamic DiD coefficients from estimating equation (6). We present the set of β_k, coefficients on the $MiningCountry_i$ dummy k months from China's ban. The dots denote point estimates and spikes 95% confidence intervals. The dependent variable is the monthly Bitcoin hashrate. The top panel presents standard DiD estimates whereas the bottom panel shows SDiD estimates. Table A.7 reports regression estimates. Results are discussed in section 5.1.3.

Figure 3: Impact of Ethereum's Transition to Proof-of-Stake on US Electricity Use

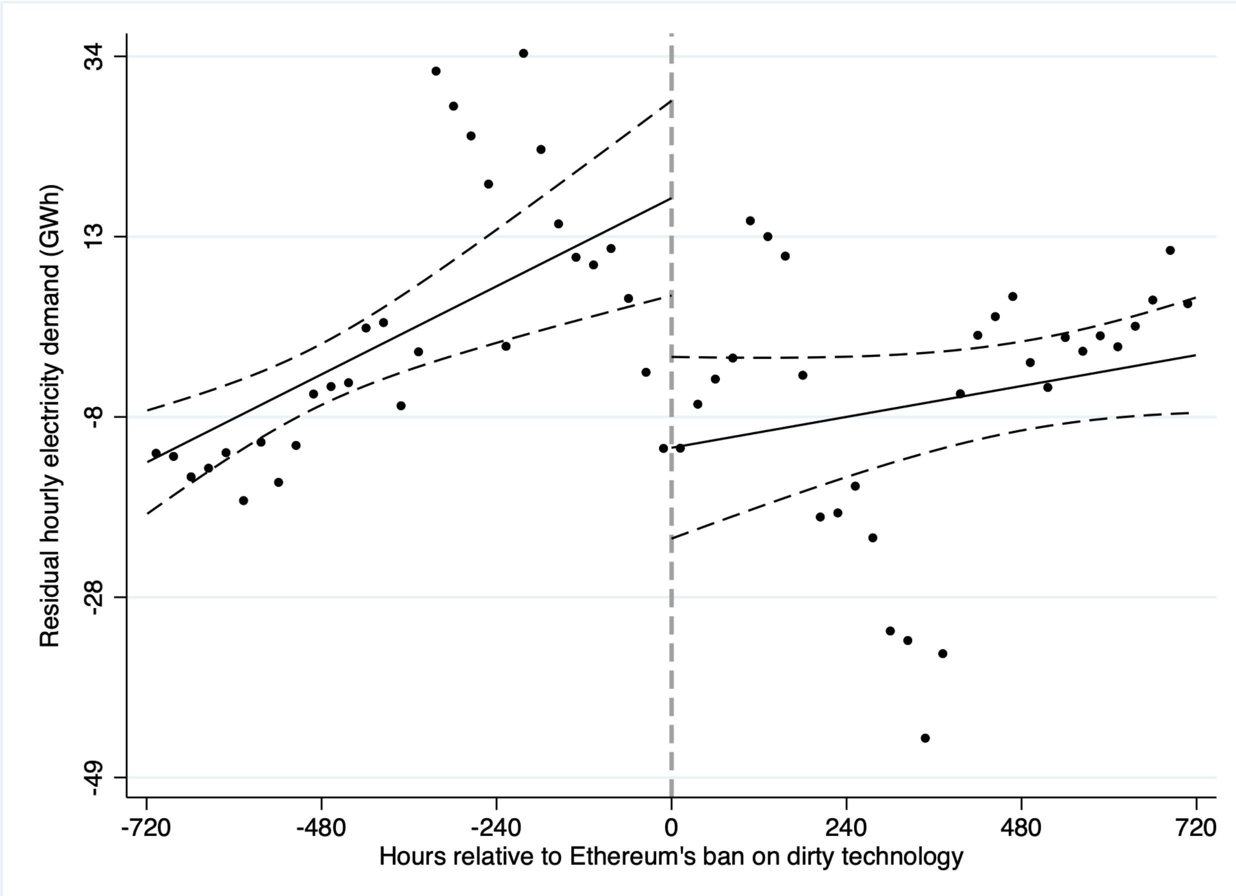

Notes: This figure plots US hourly electricity consumption residuals for 30 days before and 30 days after Ethereum's transition to PoS on 15 September 2022 at 2:45am EST. We obtain residuals by regressing electricity consumption on weather controls (5°C wide temperature bins, precipitation and its square, dew point depression, and wind speed) and time fixed effects (month-of-sample, year-by-day-of-week, federal holiday, and day-of-week-by-hour-of-day FEs) between 1 January 2021 and 31 December 2023. Dots are daily mean residuals. The solid lines are lines of best fit and the dashed lines are 95% confidence intervals, fit separately pre- and post-transition. Table 7 reports regression estimates. Results are discussed in section 6.2.

Figure 4: Impact of Ethereum's Transition to Proof-of-Stake on Hashrates of Other Cryptocurrencies, Compatible and Not-Compatible

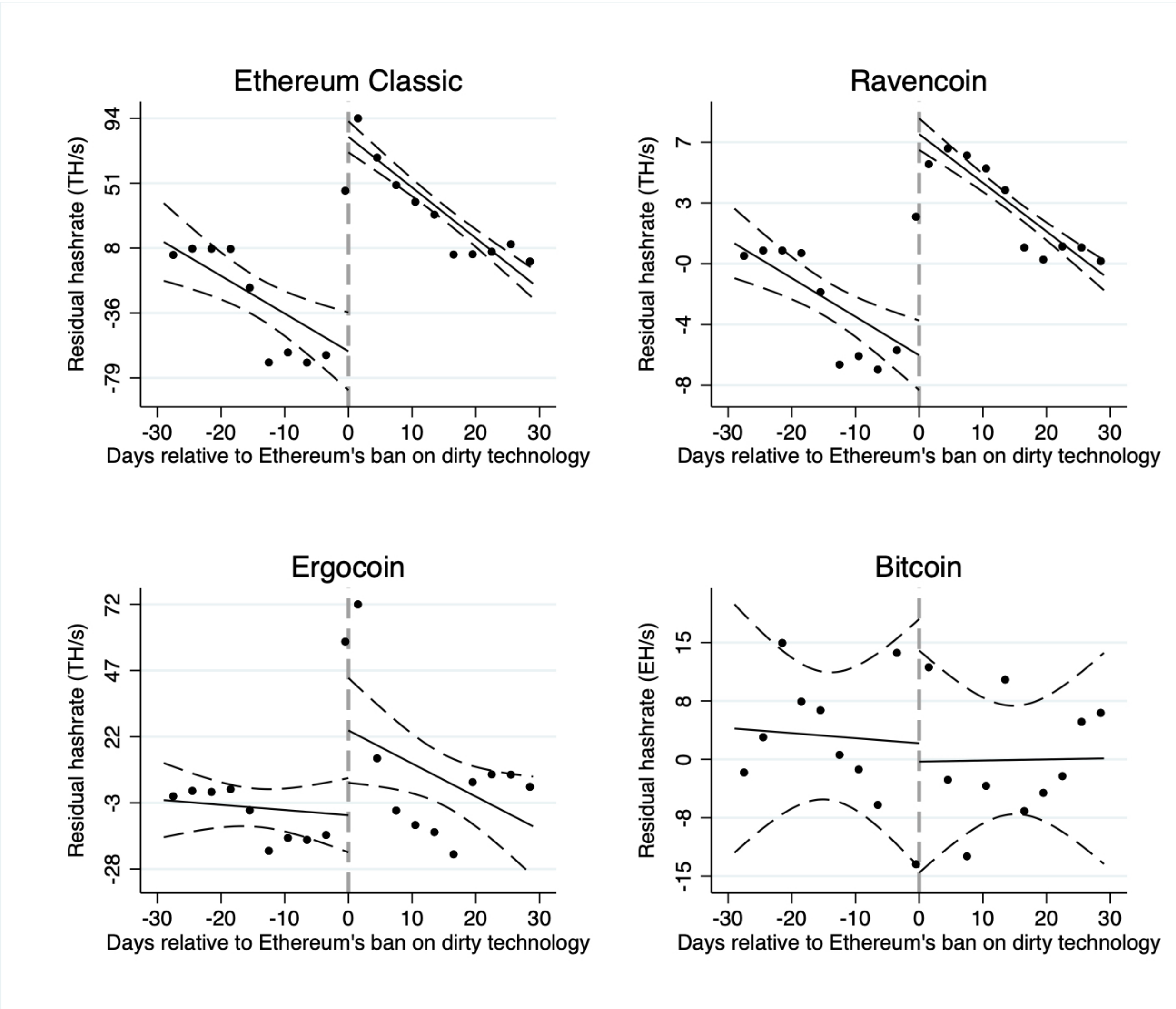

Notes: This figure plots daily hashrate (TH/s) residuals for four PoW cryptocurrencies over 30 days before and 30 days after Ethereum's transition to PoS. Like Ethereum prior to its clean technology adoption, Ethereum Classic, Ravencoin and Ergocoin are all GPU-minable, whereas Bitcoin is exclusively mined with ASICs. We obtain residuals by regressing a coin's daily hashrate on its daily closing price, weather controls (5°C wide temperature bins, precipitation and its square, dew point depression, and wind speed), and time fixed effects (month-of-sample, year-by-day-of-week fixed effects, and federal holiday) between 1 January 2021 and 31 December 2023. Dots are daily mean residuals. Dots are three-day mean residuals. The solid lines are lines of best fit and the dashed lines are 95% confidence intervals, fit separately pre and post Ethereum's transition. Results are discussed in section 6.3. Effect sizes in standard deviation terms are depicted in figure A.16.

A Appendix Tables and Figures

Table A.1: HS codes for Cryptomining Equipment in China and the US

Harmonized System (HS) codes	Export, China	Import, United States
Cryptomining machines	84715040	8543709960
Hashboards	84733090	847330 (only HS6)

Notes: We source Chinese export HS 8-digit codes for cryptomining machines and hashboards from Bitmain's website. We obtained the US import HS 10-digit code for cryptomining machines from Customs and Border Protection tariff ruling N297495, which clarified the product's tariff classification (US CBP, 2018).

Table A.2: Impacts of China's Mining Ban on COVID-19 Lockdown Measures and Nightlight Intensity

Dependent variable is:	Covid-19 Lockdown Stringency Index	Nightlight Intensity
	(1)	(2)
Mining Province × Post Ban	1.425	0.035
	(2.387)	(0.035)
Dependent variable mean prior to ban for Mining Province	20.672	0.460
Number of observations	2077	2077

Notes: This table presents results from estimating our baseline DiD regression, equation (1), replacing dependent variables with either the province-month level COVID-19 stringency index constructed by Hale et al. (2021) in column 1, or nighttime light intensity averaged across all grids within each province (column 2). Standard errors are clustered by province. Significant at *10%, **5%, and ***1%. Results are discussed in section 4.2.

Table A.3: Domestic Impacts of China's Mining Ban on Electricity Markets—Robustness to Confounding Factors

Dep. var. as indicated by panel.	(1)	(2)	(3)	(4)	(5)
Panel A. Electricity consumption (GWh)					
Mining Province × Post Ban	-1169.9*	-1127.4*	-1175.9*	-1247.2*	-1189.8*
	(669.0)	(634.3)	(668.5)	(693.4)	(661.5)
Dependent variable mean prior to ban for Mining Province	23,234.6	23,234.6	23,234.6	23,234.6	23,234.6
Number of observations	2077	2077	2077	2077	2077
Panel B. Fossil-fuel electricity generation (GWh)					
Mining Province × Post Ban	-953.3**	-943.6**	-958.2**	-874.5*	-863.3*
	(396.0)	(393.7)	(396.4)	(444.3)	(442.7)
Dependent variable mean prior to ban for Mining Province	17,260.4	17,260.4	17,260.4	17,260.4	17,260.4
Number of observations	2077	2077	2077	2077	2077
Panel C. Electricity exports (GWh)					
Mining Province × Post Ban	1679.0**	1677.4**	1679.1**	1731.5**	1730.1**
	(650.7)	(652.1)	(650.9)	(632.2)	(634.9)
Dependent variable mean prior to ban for Mining Province	11,705.4	11,705.4	11,705.4	11,705.4	11,705.4
No. of obs. (30 provinces)	2010	2010	2010	2010	2010
COVID-19 stringency control		✓			✓
Night light intensity control			✓		✓
Dual-control policy control				✓	✓

Notes: This table presents results from estimating our baseline DiD regression equation (1), adding controls for several potential confounding factors that may affect electricity markets. Column 1 reproduces the baseline estimates in tables 1 and 2. Column 2 controls for the province-by-month level COVID-19 stringency index, as constructed by Hale et al. (2021). Column 3 controls for monthly nighttime light intensity averaged across all grids within each province. Column 4 adds an interaction between (i) a dummy denoting nine provinces for which a Level I (highest) warning was issued for not delivering on their energy-intensity reduction targets and (ii) a dummy denoting June 2021 (when the warning was issued) onwards. Column 5 adds all these controls simultaneously. Standard errors are clustered by province. Significant at *10%, **5%, and ***1%. Results are discussed in sections 4.2 and 4.3.

Table A.4: Domestic Impacts of China's Mining Ban on Electricity Markets—Staggered DiD estimates

Dependent variable (in GWh):	Electricity consumption (1)	Fossil electricity generation (2)	Electricity exports (3)
Panel A. DiD			
Mining Province Post Ban	-1245.2	-1058.6*	2066.0**
	(823.5)	(571.7)	(825.6)
Panel B. SDiD			
Mining Province Post Ban	-1455.9*	-807.6	1685.5*
	(764.6)	(762.9)	(981.0)
Dependent variable mean prior to ban for Mining Province	23,049.9	16,716.8	11,530.4
Number of observations	2077	2077	2010

Notes: This table presents results from estimating our baseline DiD regression equation (1), except that the timing of treatment is allowed to vary by province. Panel A contains standard DiD estimates while panel B contains synthetic DiD estimates. Each observation is a province-month pair. The sample covers 31 provinces (and 30 provinces in column 3 due to missing electricity exports for Beijing) from January 2018 to July 2023. The dependent variable is total electricity consumption in column 1; fossil-fuel generation in column 2; and electricity exports in column 3 (all in GWh). Dummy variable *Mining Province Post Ban* takes value 1 for all months after February 2021 for Inner Mongolia, May 2021 for Xinjiang, and June 2021 for Sichuan and Yunnan. Fixed effects and controls are as in tables 1 and 2. Standard errors are clustered by province (and cluster-bootstrapped with 1000 replications in panel B). Significant at *10%, **5%, and ***1%. Results are discussed in section 4.2.

Table A.5: Impacts of China's Mining Ban on Fossil Generation—Robustness to Controlling for Hydropower Generation Capacity

Dependent variable is Fossil electricity generation (GWh)	Baseline (1)	Control hydropower capacity (2)
Panel A. DiD		
Mining Province × Post Ban	-953.3**	-1125.1***
	(396.0)	(343.9)
Panel B. Response by province		
Inner Mongolia × Post Ban	-1795.9***	-1786.4***
	(224.7)	(222.1)
Xinjiang × Post Ban	-1014.0***	-1027.8***
	(218.4)	(220.6)
Sichuan × Post Ban	-110.1	-619.2
	(255.5)	(584.1)
Yunnan × Post Ban	-902.9***	-887.0***
	(243.9)	(239.2)
Dependent variable mean prior to ban for Mining Province	17,260.4	17,260.4
Number of observations	2077	2077

Notes: This table presents results from estimating our baseline DiD regression equation (1), for monthly fossil-fuel electricity generation (GWh). Column 1 reproduces the estimate of table 2, column 1. Column 2 includes a control for province-by-year hydropower generation capacity. Standard errors are clustered by province. Significant at *10%, **5%, and ***1%. Results are discussed in section 4.3.

Table A.6: Global Spillovers of China's Mining Ban—US Imports of Cryptomining Machines

Dependent variable is Import value (million USD) from:	DiD		SDiD	
	China	World	China	World
	(1)	(2)	(3)	(4)
Mining Machine × Post Ban	39.1***	209.0***	15.4***	287.6***
	(0.9)	(9.4)	(1.7)	(15.7)
Dependent variable mean prior to ban for Mining Equipment	42.1	356.3	42.1	356.3
Number of observations	2530	2530	2530	2530

Notes: This table reports estimates of DiD coefficient β from equation (4). Columns 1-2 show standard DiD estimates and columns 3-4 show synthetic DiD estimates. An observation is a product-month pair. The sample covers all 46 HS10-digit products in NAICS industry 335999—of which cryptomining machines are one HS10 product— between January 2019 and July 2023. The dependent variable is US imports (in USD million, base January 2019) of product j in month t from China only in columns 1 and 3 and from all origin countries in columns 3 and 4. *Mining Machine* denotes cryptomining machines (HS10 code 8543709960). *Post Ban* denotes months from May 2021 onwards. All regressions include product-by-month-of-year and month-of-sample fixed effects, and product-specific time trends. Standard errors are clustered by product (and we conduct placebo inference with 1000 replications in columns 3-4). Significant at *10%, **5%, and ***1%. Results are discussed in section 5.1.2 and further presented figures A.9 and A.11.

Table A.7: Global Spillovers of China's Mining Ban—Impacts on Bitcoin Mining Activity and Electricity Consumption in Other Countries

Dependent variable is	Bitcoin hashrate (EH/s)	Electricity consumption (GWh)
	(1)	(2)
Panel A. Effect on major cryptomining countries		
Mining Country × Post Ban	4.5	2974
	(3.8)	(2202)
Dep.var. mean pre-ban for Mining Country	5.9	130,142
Panel B. Effect on US and other major cryptomining countries		
United States × Post Ban	21.6***	8034***
	(0.0)	(186)
Other Mining Countries × Post Ban	1.0	445
	(2.4)	(756)
Dep.var. mean pre-ban for US	10.2	331,013
Dep.var. mean pre-ban for non-US mining countries	5.0	29,706
Number of observations	2204	2479

Notes: This table presents estimates from equation (6). An observation is a country-month pair. In column 1, the dependent variable is the Bitcoin hashrate (EH/s) and the sample covers 76 countries from September 2019 to January 2022. In column 2, the dependent variable is total electricity consumption (GWh) and the sample covers 37 countries from January 2018 to July 2023. See sections 3.1 and 3.2 for data limitations and sampling choices. In panel A, dummy *Mining Country* indicates major cryptomining countries other than China before the ban, and is 1 for the US, Malaysia, Kazakhstan, Canada, Russia, and Iran. In column 2, the indicator denotes the US, Canada, and Malaysia, since monthly electricity consumption for Kazakhstan, Russia, and Iran are missing. In panel B, *Other Mining Countries* excludes the US. Dummy *Post Ban* denotes months from May 2021 onwards. All regressions include country-by-month-of-year and month-of-sample fixed effects, and country-specific time trends. Standard errors are clustered by country. Significant at *10%, **5%, and ***1%. Results are discussed in sections 5.1.3 and 5.2 and further presented in figure 2.

Table A.8: Impacts of China's Mining Ban on Electricity Consumption in US Mining States—Robustness Tests

Dependent variable is Electricity consumption (GWh)	All sectors (1)	Commercial/Industrial (2)	Residential (3)
Panel A. Baseline			
Mining State × Post Ban	415.6***	514.9**	-103.1
	(141.0)	(195.6)	(63.9)
Panel B. Control COVID-19			
Mining State × Post Ban	416.7***	513.8**	-100.7
	(142.5)	(197.6)	(63.6)
Panel C. Control Night Light Intensity			
Mining State × Post Ban	415.1***	514.3**	-103.1
	(141.2)	(195.8)	(63.9)
Panel D. Control Texas Freeze			
Mining State × Post Ban	371.5***	478.7**	-111.1*
	(122.2)	(184.0)	(66.2)
Panel E. Classify California as a Non-Mining State			
Mining State × Post Ban	312.9**	338.7*	-28.0
	(145.7)	(175.6)	(33.2)
Dependent variable mean prior to ban for Mining State	17,103.1	10,688.2	6351.8
Dependent variable mean prior to ban for Mining State (excluding California)	16,210.1	10,070.2	6075.4
Number of observations	3216	3216	3216

Notes: This table shows estimates of the ban's impact on US electricity consumption, adding controls for several potential confounding factors. Panel A reproduces estimates from table 5, panel A. Panel B additionally controls for the state-month level COVID-19 stringency index, as constructed by Hale et al. (2021). Panel C controls for monthly nighttime light intensity averaged across all grids within each state. Panel D includes a dummy variable that equals one for Texas in February 2021 to account for the power crisis caused by the Great Texas Freeze. In panel E, we no longer model California as a major cryptomining state, i.e., *Mining State* here refers only to the four states Texas, Georgia, New York, and Kentucky, rather than the baseline five including California. An observation is a US state-month pair. The dependent variable (in GWh) is electricity consumption across all sectors in column 1, in the commercial and industrial sectors only in column 2, and in the residential sector only in column 3. Other notes are the same as table 5. Standard errors are clustered by state. Significant at *10%, **5%, and ***1%. Results are discussed in section 5.2.

Table A.9: Global Spillovers of China's Mining Ban—Impacts on Electricity Generation in Other Countries

Dependent variable is Electricity generation (GWh)	All sources (1)	Fossil (2)	Non-fossil (3)
Panel A. Effect on major cryptomining countries			
Mining Country × Post Ban	4060	5425**	1725
	(3121)	(2579)	(1899)
Pre-ban depvar mean for Mining Country	102,672	93,235	70,273
Panel B. Effect on US and other major cryptomining countries			
United States × Post Ban	17,203***	10,998***	6205***
	(219)	(215)	(91)
Other Mining Country × Post Ban	774	2638	-514
	(957)	(1599)	(356)
Dep.var. mean pre-ban for US	344,640	212,172	132,468
Dep.var. mean pre-ban for Other Mining Country	42,180	33,767	39,176
Number of countries	49	47	47
Number of observations	3283	3149	3149

Notes: This table presents estimates from equation (6). An observation is a country-month pair, and the sample contains 49 countries that report electricity generation between January 2018 and July 2023. The dependent variable is electricity generation (GWh) across all energy sources in column 1, only fossil fuels in column 2, and only non-fossil sources (hydroelectric, wind, nuclear, and solar) in column 3. In panel A, *Mining Country* refers to five countries with significant cryptomining activity for which monthly electricity generation data are available (US, Canada, Malaysia, Russia, Kazakhstan; for Malaysia and Kazakhstan, only total generation is available). In panel B, *Other Mining Countries* refer to these major cryptomining countries except the US. *Post Ban* denotes months from May 2021 onwards. All regressions include country-by-month-of-year and month-of-sample fixed effects, and country-specific time trends. Standard errors are clustered by country. Significant at *10%, **5%, and ***1%. Results are discussed in section 5.2.

Table A.10: Global Spillovers of China's Mining Ban—Impacts on Electricity Generation in US Mining States

Dependent variable is Electricity generation (GWh)	All sources (1)	Fossil (2)	Non-fossil (3)
Panel A. DiD			
Mining State × Post Ban	341.8	411.2***	-69.4
	(298.1)	(104.8)	(241.0)
Panel B. SDiD			
Mining State × Post Ban	814.1	647.2*	148.8
	(554.4)	(356.9)	(335.1)
Panel C. Response by US state (DiD)			
Texas × Post Ban	1379.9***	718.8***	661.1***
	(66.9)	(71.1)	(29.6)
Georgia × Post Ban	101.0	179.2**	-78.2**
	(71.9)	(73.3)	(30.9)
New York × Post Ban	-554.1***	367.7***	-921.8***
	(68.1)	(69.1)	(32.2)
Kentucky × Post Ban	355.6***	461.6***	-106.0***
	(69.7)	(70.8)	(28.1)
California × Post Ban	427.2***	327.7***	99.4***
	(68.9)	(67.8)	(36.2)
Dependent variable mean prior to ban for Mining State	16,533.4	10,379.2	6154.2
Number of observations	3216	3216	3216

Notes: This table presents results for DiD regressions akin to equation (6). Panels A and C report standard DiD estimates while panel B reports synthetic DiD estimates. An observation is a US state-month pair, and the sample covers the 48 US contiguous from January 2018 to July 2023. The dependent variable is electricity generation (GWh) across all energy sources in column 1, only fossil fuels in column 2, and only non-fossil sources (hydroelectric, wind, nuclear, and solar) in column 3. *Mining State* is a dummy for the five major US cryptomining states prior to China's ban (Texas, Georgia, New York, Kentucky, and California). *Post Ban* denotes months from May 2021 onwards. All regressions include state-by-month-of-year and month-of-sample fixed effects, state-specific time trends, and weather controls (as in table 1). Standard errors are clustered by province in panels A and C and cluster-bootstrapped with 1000 replications in panel B. Significant at *10%, **5%, and ***1%. Results are discussed in section 5.2.

Table A.11: Impacts of China's Mining Ban on Electricity Generation in US Mining States—Robustness Tests

Dependent variable is Electricity generation (GWh)	All sources (1)	Fossil (2)	Non-fossil (3)
Panel A. Baseline			
Mining State × Post Ban	341.8	411.2***	-69.4
	(298.1)	(104.8)	(241.0)
Panel B. Control COVID-19			
Mining State × Post Ban	334.2	414.5***	-80.3
	(302.1)	(105.4)	(245.8)
Panel C. Control Night Light Intensity			
Mining State × Post Ban	342.5	412.2***	-69.7
	(297.6)	(104.4)	(240.8)
Panel D. Control Texas Freeze			
Mining State × Post Ban	305.7	432.8***	-127.1
	(274.8)	(120.0)	(207.8)
Panel E. Classify California as a Non-Mining State			
Mining State × Post Ban	310.8	424.5***	-113.7
	(368.6)	(119.6)	(295.5)
Dependent variable mean prior to ban for Mining State	16,533.4	10,379.2	6154.2
Dependent variable mean prior to ban for Mining State (excluding California)	16,634.3	11,102.4	5531.9
Number of observations	3216	3216	3216

Notes: This table shows estimates of the ban's impact on US electricity generation, adding controls for potential confounding factors. Panel A reproduces estimates from table A.10, panel A. Panel B additionally controls for the state-month level COVID-19 stringency index, as constructed by Hale et al. (2021). Panel C controls for monthly nighttime light intensity averaged across all grids within each state. Panel D includes a dummy that equals one for Texas in February 2021 to account for the power crisis caused by the Great Texas Freeze. In panel E, we no longer model California as a major cryptomining state, i.e., *Mining State* here refers only to the four states Texas, Georgia, New York, and Kentucky, rather than the baseline five including California. An observation is a US state-month pair. The dependent variable (in GWh) is electricity generation across all energy sources in column 1, only fossil fuels in column 2, and only non-fossil sources (hydroelectric, wind, nuclear, and solar) in column 3. Standard errors are clustered by state. Significant at *10%, **5%, and ***1%. Other notes are the same as table A.10. Results are discussed in section 5.2.

Table A.12: Global Spillovers of China's Mining Ban—Impacts on US Fossil-fuel Electricity Generation, Robustness Tests

	Electricity generation (GWh)			Daily average operating hours		
	All fossil	Primary fuel type		All fossil	Primary fuel type	
	plants	Coal	Gas	plants	Coal	Gas
	(1)	(2)	(3)	(4)	(5)	(6)
Panel A. Only Including Months when Plants are Active						
Mining State × Older Plant × Post Ban	11.06	58.95**	-3.54	0.31	1.91**	-0.18
	(6.87)	(25.87)	(6.29)	(0.28)	(0.90)	(0.29)
Older Plant × Post Ban	-18.86***	-33.35***	-4.37	-0.47***	-0.69*	0.02
	(4.05)	(12.84)	(3.16)	(0.15)	(0.35)	(0.16)
Mining State × Post Ban	-11.00**	-20.20	5.79	-0.24	-1.02	0.29
	(5.11)	(26.19)	(4.67)	(0.22)	(0.69)	(0.23)
Dependent variable mean prior to ban for plants in Mining State	151.84	483.56	117.64	9.08	16.73	8.30
Number of observations	71,547	14,827	56,710	71,579	14,839	56,730
Panel B. Classify California as a Non-Mining State						
Mining State × Older Plant × Post Ban	-0.55	53.06**	-12.87**	0.22	1.86**	-0.16
	(6.56)	(24.29)	(6.26)	(0.33)	(0.92)	(0.35)
Older Plant × Post Ban	-16.70***	-30.02**	-3.19	-0.51***	-0.72	-0.01
	(3.63)	(12.82)	(3.05)	(0.15)	(0.45)	(0.15)
Mining State × Post Ban	-1.57	-11.12	9.52	-0.30	-0.64	0.05
	(6.29)	(23.78)	(5.80)	(0.28)	(0.78)	(0.29)
Dependent variable mean prior to ban for plants in Mining State	172.99	424.68	132.85	9.40	14.70	8.56
Number of observations	79,453	16,161	63,292	79,485	16,173	63,312
Panel C. Cluster Standard Errors at State Level						
Mining State × Older Plant × Post Ban	11.72	53.06*	-2.22	0.44	1.86***	-0.03
	(9.78)	(30.73)	(8.31)	(0.32)	(0.66)	(0.36)
Older Plant × Post Ban	-20.15***	-30.02*	-5.32	-0.58***	-0.72	-0.04
	(5.91)	(16.08)	(4.22)	(0.19)	(0.60)	(0.20)
Mining State × Post Ban	-9.83	-11.12	6.28	-0.25	-0.64	0.32
	(7.09)	(14.35)	(7.37)	(0.33)	(0.71)	(0.41)
Dependent variable mean prior to ban for plants in Mining State	137.80	424.68	107.09	8.24	14.70	7.55
Number of observations	79,453	16,161	63,292	79,485	16,173	63,312

Notes: This table shows three robustness checks on estimates from equation (7). The dependent variable is either electricity generation (column 1-3) or daily average operating hours (column 4-6) of power plant i in month t. An observation is a plant-month pair, and the time period of analysis is January 2018 to July 2023. In panel A, the sample is restricted to active months where plants have non-zero electricity generation. In panel B, we do not model California as a major cryptomining state, i.e., *Mining State* refers only to four states Texas, Georgia, New York, and Kentucky, rather than the baseline five states including California. In panel C, we cluster standard errors by state. Other notes are the same as in table 6. Results are discussed in section 5.2.3. Baseline results on fossil plant responses are in table 6.

Table A.13: Net Impacts of Mining Ban on Chinese and US Electricity Consumption & Generation

Dependent variable:	Electricity consump. (GWh)	Electricity generation (GWh)	
		Total	Fossil
	(1)	(2)	(3)
Mining Location × Post Ban × China	-1692.1**	-271.4	-1420.9***
	(676.4)	(751.2)	(403.0)
Mining Location × Post Ban	418.7***	337.9	426.0***
	(133.7)	(293.5)	(111.2)
Post Ban × China	311.7	-203.5	-283.1
	(192.3)	(232.5)	(243.8)
Dependent var. mean prior to ban for Mining Location	19,828.2	23,748.3	13,437.5
Dependent var. mean prior to ban for all locations	11,619.5	11,784.2	8081.3
Number of locations	79	79	79
Number of observations	5293	5293	5293

Notes: This table shows estimates from equation (8). An observation is a subnational unit-month pair. The sample covers 31 Chinese provinces and 48 contiguous US states (i.e., 79 units) between January 2018 and July 2023. The dependent variable (GWh) is total electricity consumption in column 1, total electricity generation in column 2, and fossil-fuel generation in column 3. *Mining Location* denotes US states or Chinese provinces with significant cryptomining activity before China's ban, i.e., four Chinese provinces and five US states as in the foregoing analysis. *China* is a dummy that takes value 1 for all Chinese provinces. *Post Ban* denotes months from May 2021 onwards. All regressions include location-by-month-of-year and month-of-sample fixed effects, province/state-specific time trends, and weather controls (as in table 1). Standard errors are clustered by location. Significant at *10%, **5%, and ***1%. Results are discussed in section 5.3. Baseline DiD estimates of the ban's impact on Chinese consumption and generation are in tables 1 and 2, while estimates of impacts on US consumption and generation are in tables 5 and A.10, respectively.

Table A.14: Impact of Ethereum's Transition on US Electricity Consumption—Robustness Tests

	Dependent variable: Hourly electricity consumption (GWh)				
	Baseline	Only control for time FE	Control 24-hour lag of weather controls	"Donut"-test: Remove X days around PoW ban	
				X=1	X=3
	(1)	(2)	(3)	(4)	(5)
Post Ethereum Transition	-16.6***	-24.0**	-16.4***	-20.3***	-28.0***
	(3.9)	(10.9)	(3.3)	(4.2)	(4.1)
Dependent variable mean 30 days prior to PoW ban	518.0	518.0	518.0	519.5	522.0
Number of observations	1439	1439	1439	1390	1294

Notes: This table shows estimates from our RDiT specification based on equation (10). The dependent variable is US hourly electricity consumption across all sectors (GWh) during an hour on a date between 1 January 2021 and 31 December 2023. *Post Ethereum Transition* is a dummy for all hours after 2:45am EST on 15 September 2022. Column 1 reproduces table 7, column 1, which specifies a 30-day bandwidth. Column 2 controls only for time fixed effects (month-of-sample, year-by-day-of-week, federal holiday, and day-of-week-by-hour-of-day fixed effects) and does not include weather controls. Column 3 controls for the 24-hour lag of weather controls. Columns 4 and 5 remove observations right around the cutoff: +/- 1 day and +/- 3 days, respectively. Standard errors are bootstrapped at the date level with 500 replications. Significant at *10%, **5%, and ***1%. Results are discussed in section 6.

Figure A.1: Ethereum's Daily Hashrate Before vs After its Transition to Proof-of-Stake

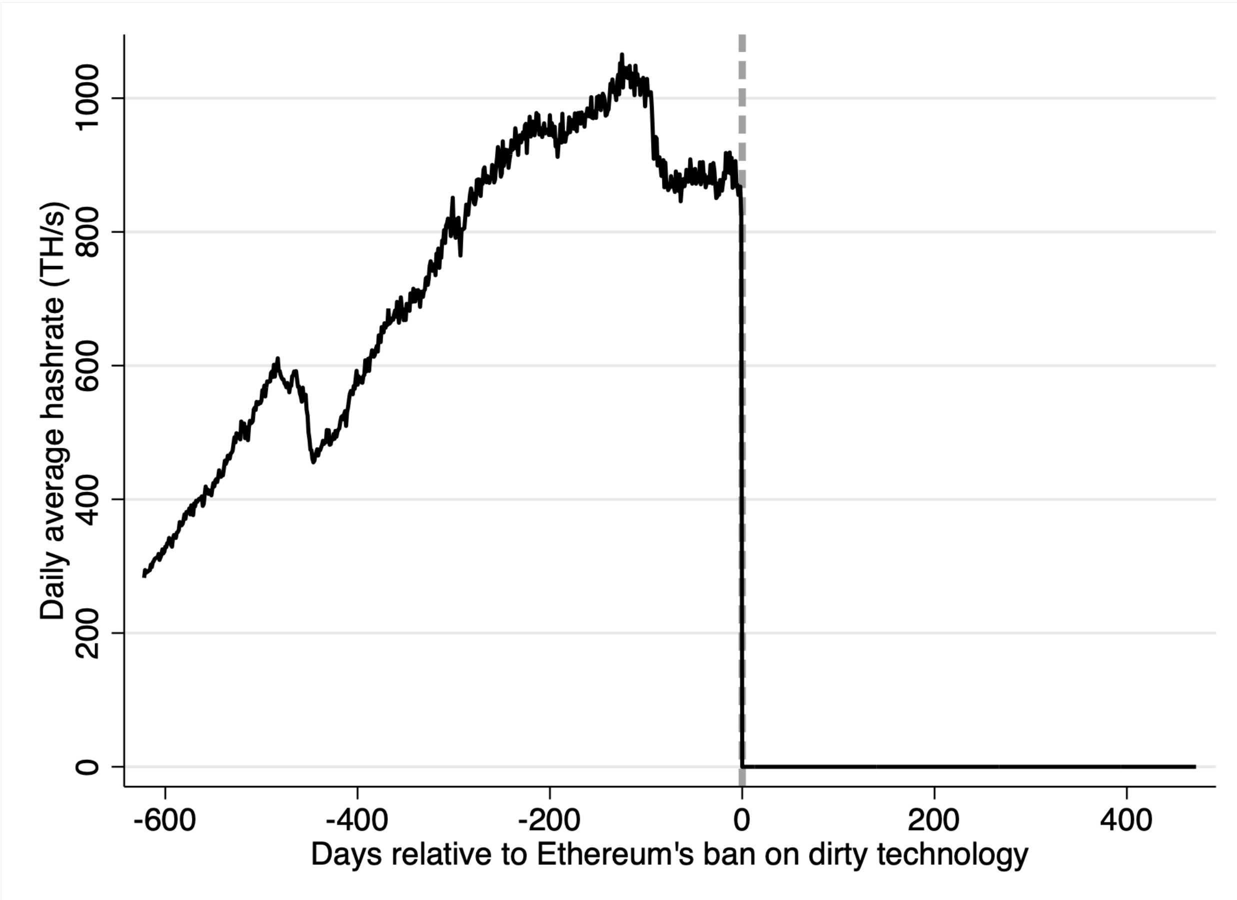

Notes: This figure displays daily Ethereum hashrates between January 2021 (about 600 days before Ethereum's transition) and December 2023 (nearly 500 days after the transition). The vertical line marks 15 September 2022, when Ethereum transitioned to PoS, officially ending PoW mining operations on its network. Data is from CoinMetrics. Results are discussed in section 6.1.

Figure A.2: Validating Mining Activity Data—Aggregated CCAF vs Network-wide CoinMetrics Hashrates

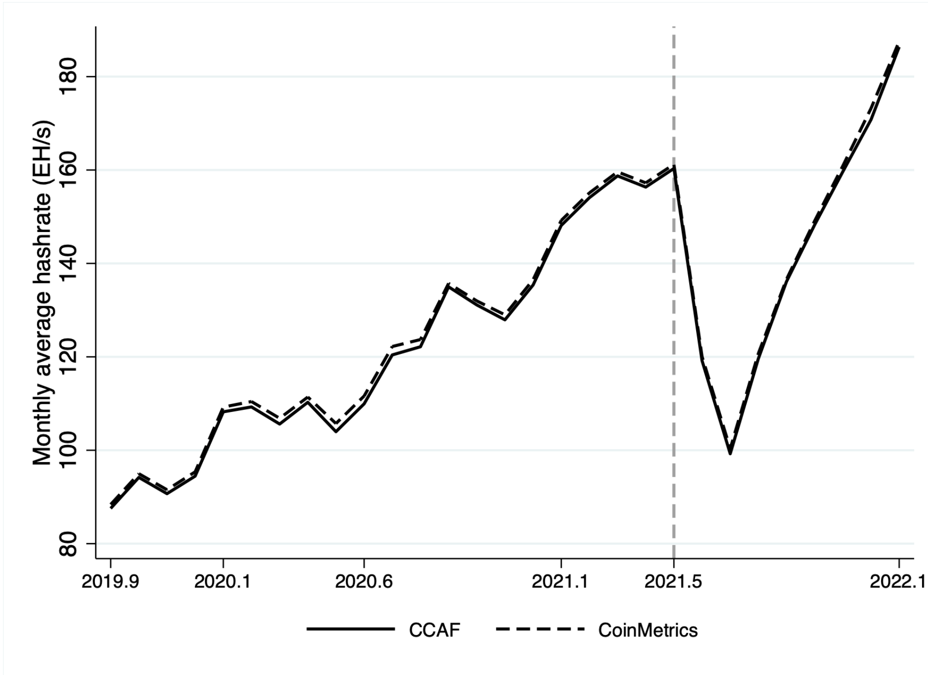

Notes: This figure shows trends in monthly hashrates from (i) our data, which comes from the Cambridge Centre for Alternative Finance (CCAF) and (ii) Bitcoin network-wide hashrate from CoinMetrics, one of the largest cryptocurrency exchanges. For CCAF data, we aggregate the country-level hashrate for each month. For CoinMetrics data, we average the daily network hashrate over days within each month. Results are discussed in section 3.1.

Figure A.3: Global Distribution of Bitcoin Mining Activity prior to China's Ban

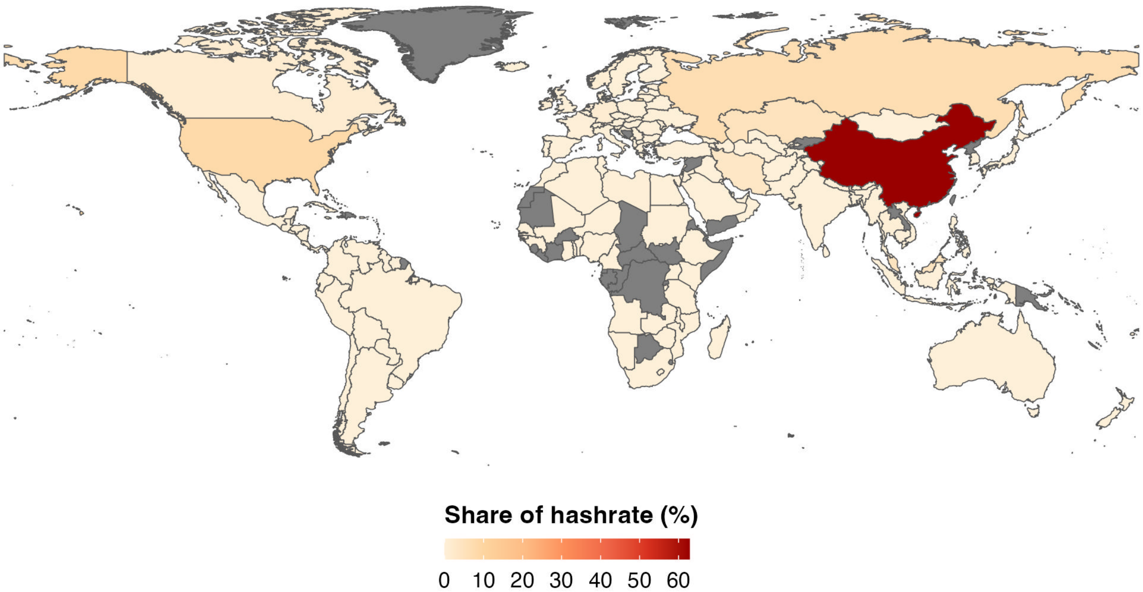

Notes: This map shows each country's share of the global Bitcoin hashrate averaged over months between September 2019 and May 2021. Data come from the Cambridge Centre for Alternative Finance (section 3.1). Gray regions indicate missing data.

Figure A.4: Distribution Within China of Bitcoin Mining Activity prior to China's Ban

(**a**) Hashrate share in the wet season

(**b**) Hashrate share in the dry season

Notes: The maps show provincial shares of the Bitcoin hashrate prior to the ban, averaged over the wet season (June to August 2020) in the top panel and over the dry season (November to January 2019/20 and 2020/21) in the bottom panel. (Hashrate data start in September 2019.) The four provinces with the largest mining shares are Xinjiang (northwest), Inner Mongolia (north), Sichuan (centre), and Yunnan (south). Data come from the Cambridge Centre for Alternative Finance (section 3.1).

Figure A.5: Global Distribution of Bitcoin Mining Activity

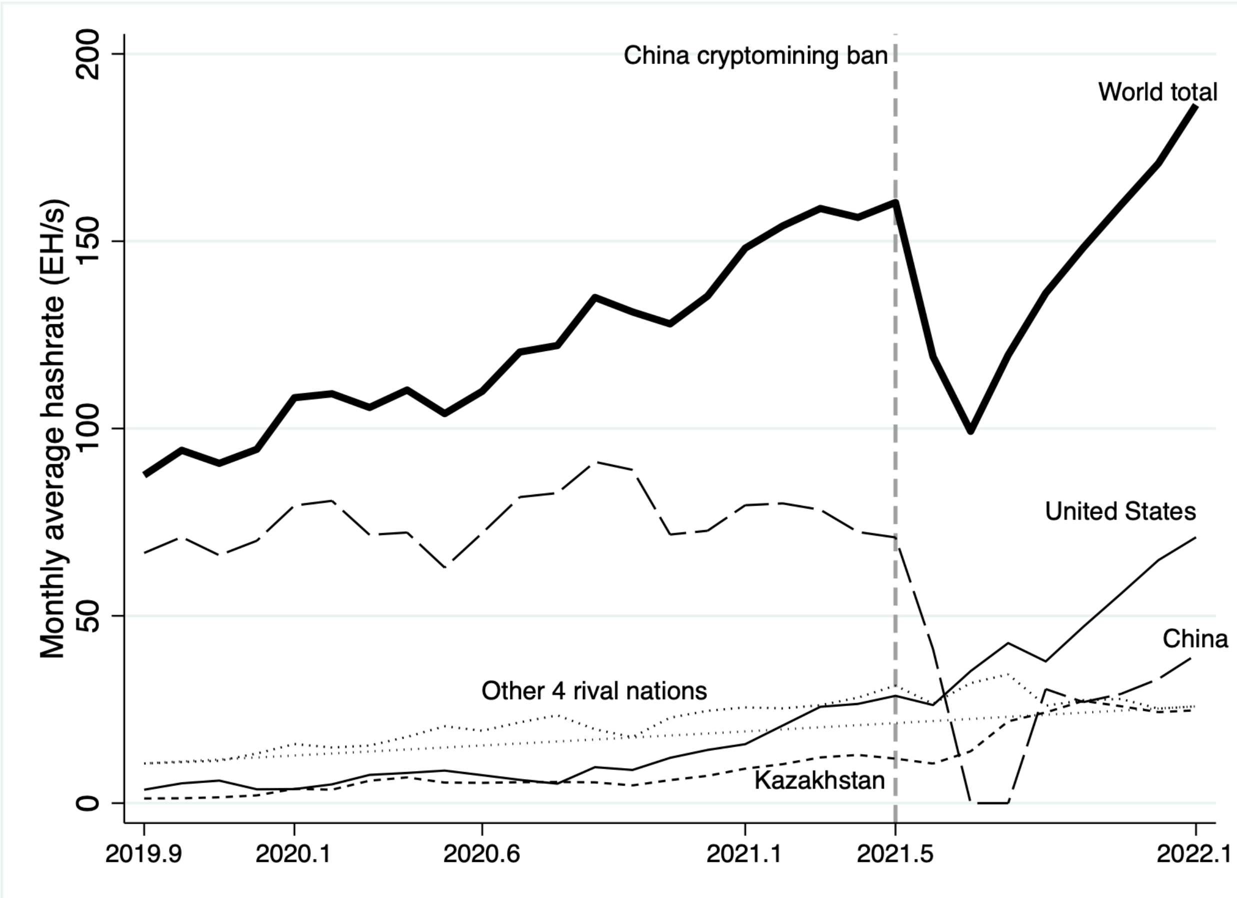

Notes: This figure displays monthly average Bitcoin hashrates in the main mining countries. The vertical line marks May 2021, when China banned cryptomining. The Bitcoin hashrate is expressed in exahashes per second (EH/s; 1 EH = 10^{18} hashes). "Other 4 rival nations" refer to the combined hashrates of Canada, Russia, Malaysia, and Iran. Data is from the Cambridge Centre for Alternative Finance and is described in section 3.1.

Figure A.6: Domestic Impacts of China's Mining Ban—Renewable Electricity Generation

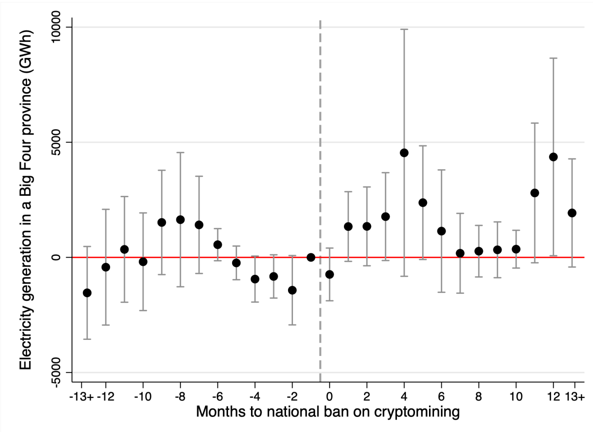

(**a**) DiD: Hydroelectric generation

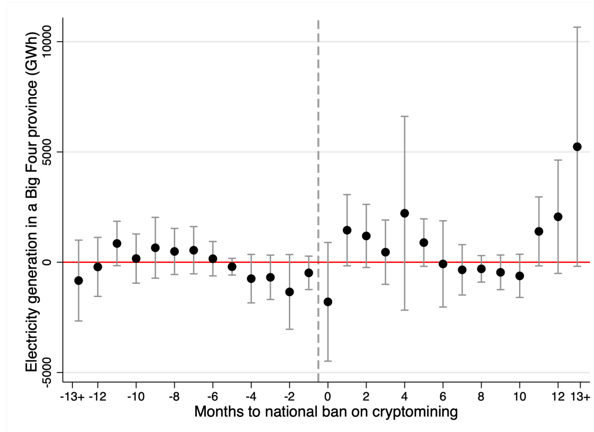

(**b**) SDiD: Hydroelectric generation

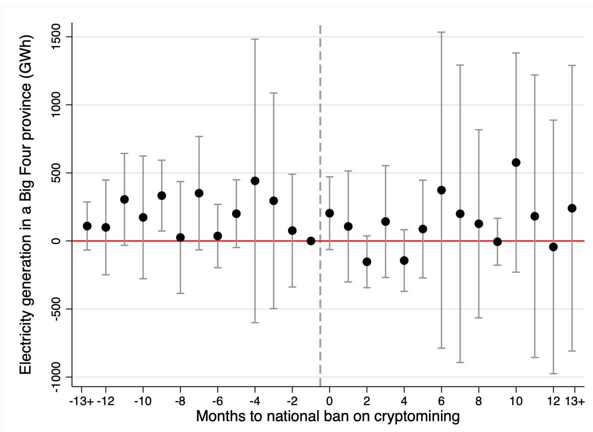

(**c**) DiD: Wind generation

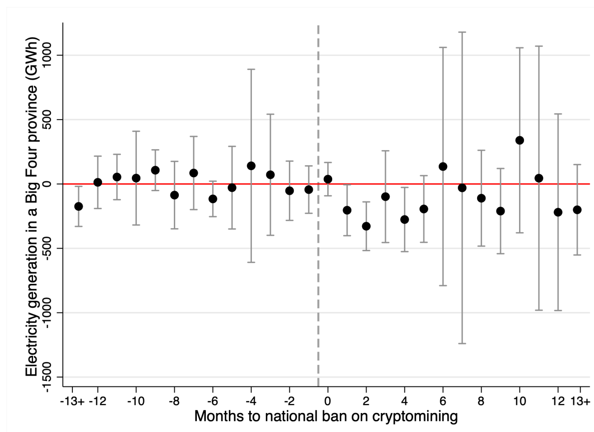

(**d**) SDiD: Wind generation

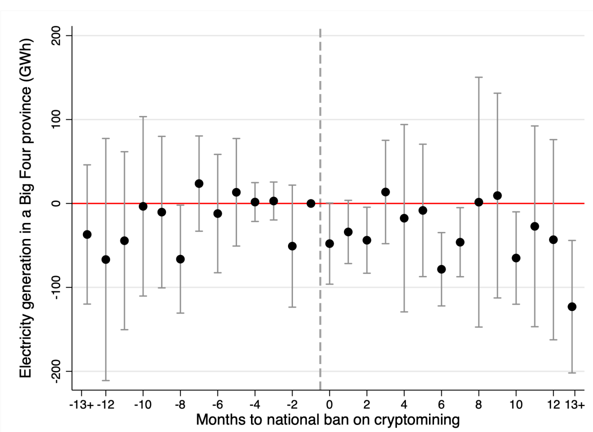

(**e**) DiD: Solar generation

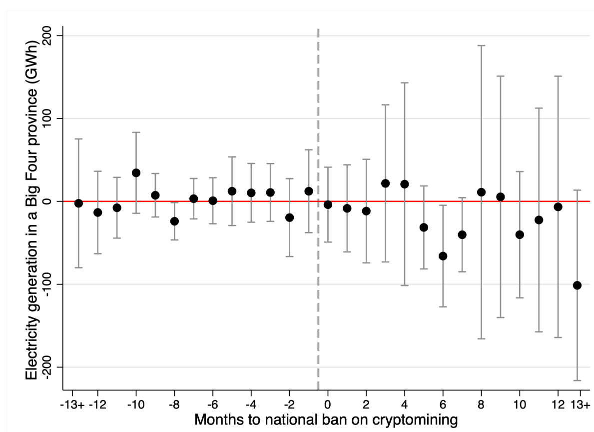

(**f**) SDiD: Solar generation

Notes: These figures show dynamic DiD coefficients from estimating equation (2). We present the set of β_k, coefficients on the $MiningProvince_i$ dummy k months from China's ban. The dots denote point estimates and spikes 95% confidence intervals. The dependent variable is hydroelectric electricity generation in panels (a)-(b), wind generation in panels (c)-(d), and solar generation in panels (e)-(f). Table 2 reports regression estimates. Results are discussed in section 4.3.

Figure A.7: Impact of China's Mining Ban on Domestic Fossil-Fuel Electricity Generation by Dry vs Wet Season

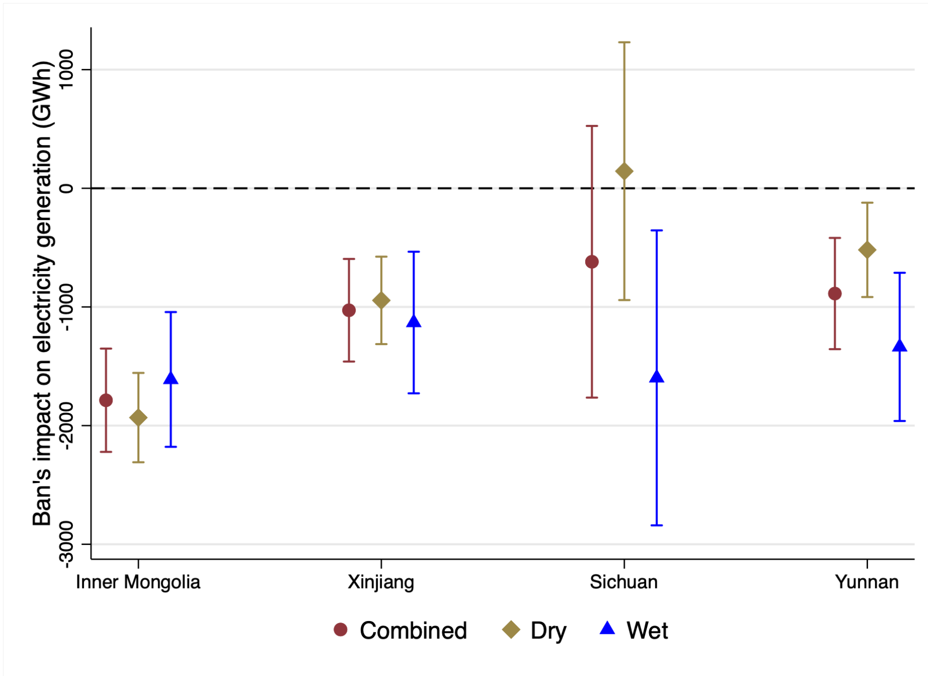

Notes: This figure reports estimates of the impact of China's cryptomining ban on domestic electricity generation based on fossil fuels. The data is at province-month level, covering January 2018 to July 2023 for 31 provinces. The combined estimates across both wet and dry seasons are based on our baseline DiD specification, equation (1). The dry season and wet season estimates come from a modified version of equation (1): $Y_{it} = \beta_1 MiningProvince_i \times Post_t \times Dry_t + \beta_2 MiningProvince_i \times Post_t \times Wet_t + X_{it}^{\prime}\Gamma + \alpha_i + \alpha_t + \epsilon_{it}$. All regressions include province-by-month-of-year and month-of-sample fixed effects, province-specific time trends, weather controls, and province-year installed hydropower capacity. Standard errors are clustered by province. The dots denote point estimates and spikes 95% confidence intervals. Results are discussed in section 4.3. Baseline DiD estimates are in table 2.

Figure A.8: Domestic Impacts of China's Mining Ban—Total Electricity Generation and Exports

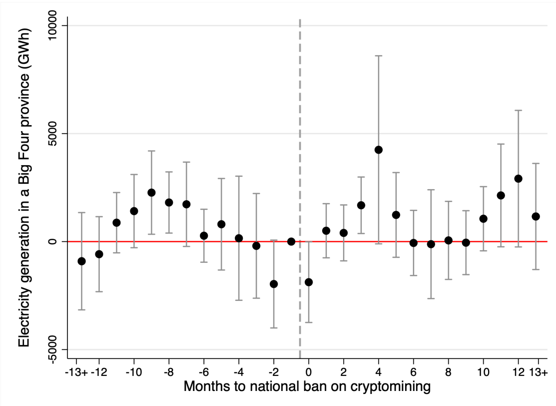

(**a**) DiD: Total electricity generation

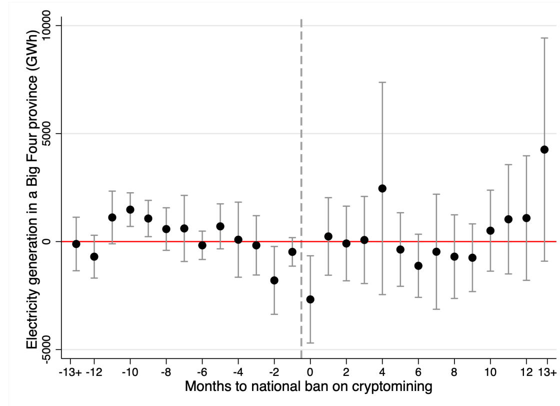

(**b**) SDiD: Total electricity generation

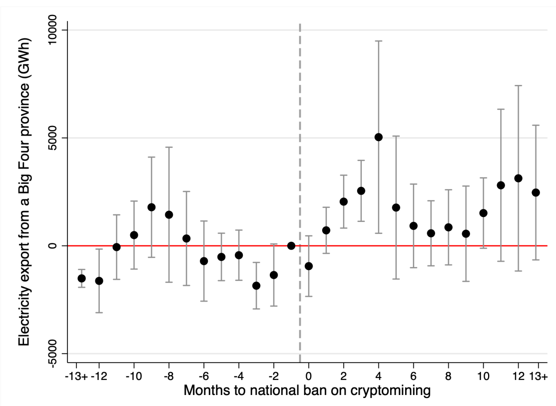

(**c**) DiD: Electricity exports

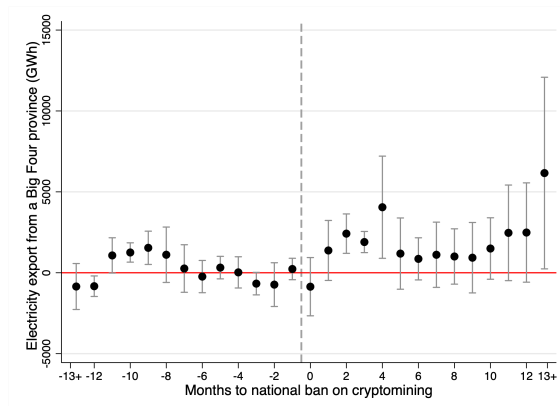

(**d**) SDiD: Electricity exports

Notes: These figures show dynamic DiD coefficients from estimating equation (2). We present the set of β_k, coefficients on the $MiningProvince_i$ dummy k months from China's ban. The dots denote point estimates and spikes 95% confidence intervals. The dependent variable is electricity generation from all energy sources in panels (a)-(b) and inter-provincial electricity transmission in panels (c)-(d). Table 2 reports regression estimates. Results are discussed in section 4.3.

Figure A.9: International Relocation of Cryptomining Equipment after China's Ban

(**a**) Chinese export of cryptomining equipment to Big Six rival nations vs other nations

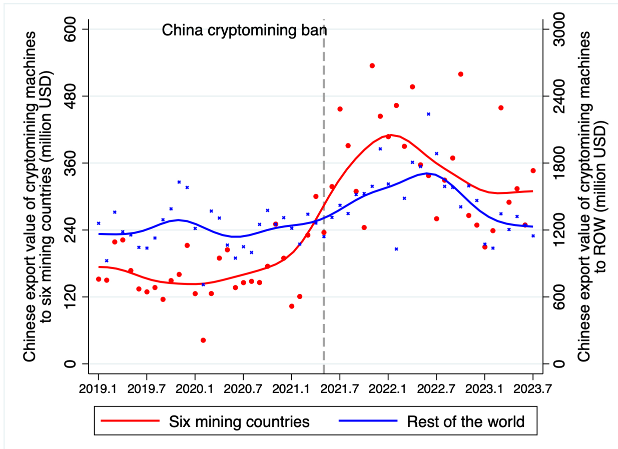

(**b**) US national import of cryptomining machines vs other products in same industry

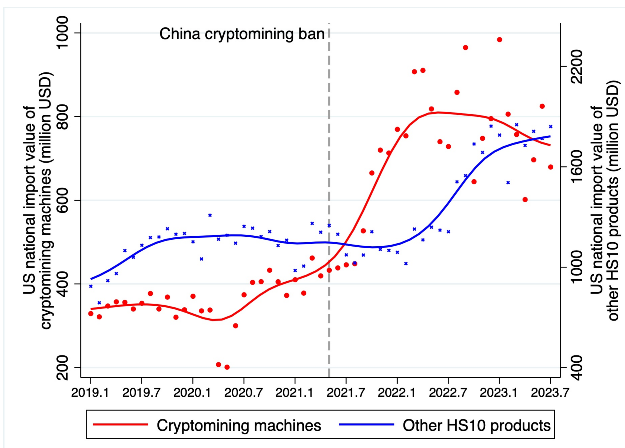

(**c**) US import of cryptomining equipment by cryptomining states vs other states

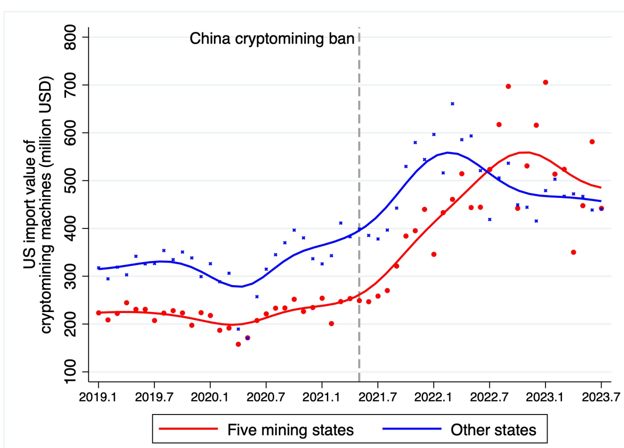

Notes: This figure illustrates trade in cryptomining equipment. The top panel shows China's monthly export value of cryptomining machines (HS8 code 84715040) to mining countries and to the rest of the world. The middle panel shows US monthly imports (from all countries) of cryptomining machines (HS10 code 8543709960) vs other HS10 products in NAICS industry 335999. The bottom panel shows US monthly imports of cryptomining machines (HS6 code 854370) by US mining vs non-mining states. Dots are raw data. Lines are local polynomial trends with a 3-month bandwidth. Results are discussed in section 5, and DiD estimates are in tables 3, A.6, and 4.

Figure A.10: Impact of China's Mining Ban on International Trade in Cryptomining Equipment—Triple Difference estimates

(**a**) Chinese exports of cryptomining equipment to the US

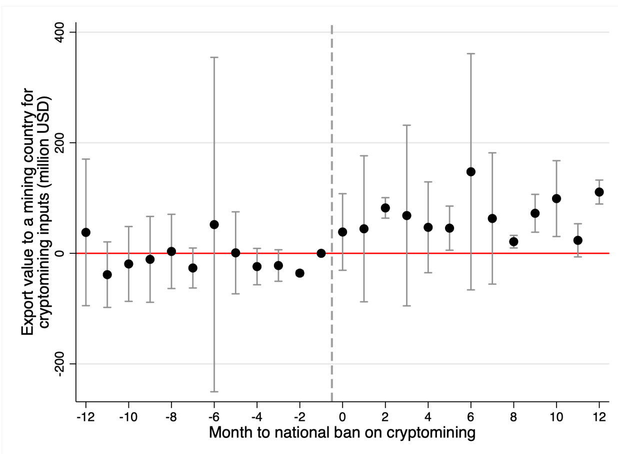

(**b**) Chinese exports of cryptomining equipment to non-US mining countries

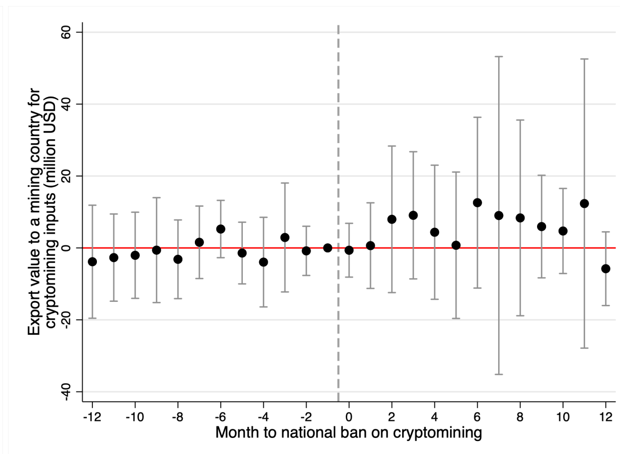

(**c**) Imports of all cryptomining equipment by US mining states

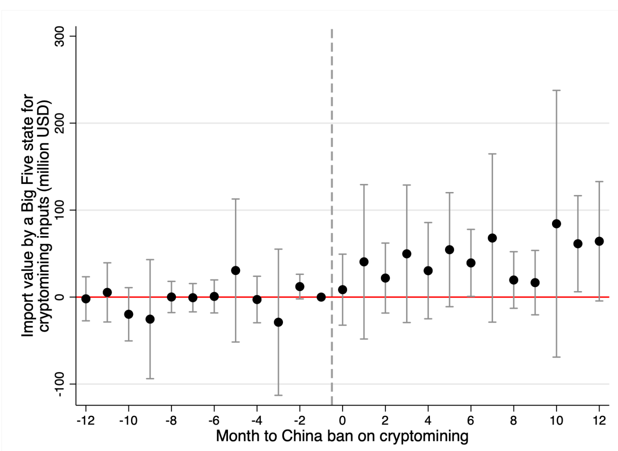

(**d**) Imports of mining machines by US mining states

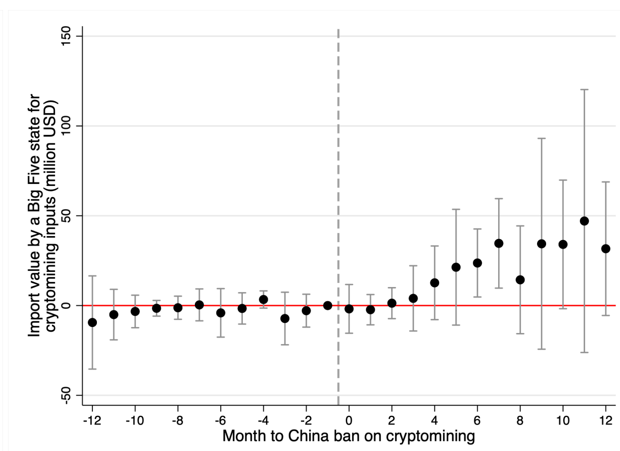

Notes: This figure shows dynamic triple-difference estimates from equation (3). The top panels present the impact of China's cryptomining ban on the monthly value of Chinese exports of cryptomining equipment (machines and hashboards) relative to other products in the same HS8 category. Panel (a) shows Chinese exports to the US whereas panel (b) shows Chinese exports to the other five major mining countries (Malaysia, Kazakhstan, Canada, Russia, and Iran). The bottom panels present the impact of China's ban on monthly imports of cryptomining equipment by the five major US mining states (Texas, Georgia, New York, Kentucky, and California). Panel (c) show all cryptomining inputs whereas panel (d) restricts to just cryptomining machines. The dots denote point estimates and spikes 95% uniform confidence intervals obtained by 9999 bootstrap repetitions. Results are discussed in section 5.1.2 and table estimates are in panel B of tables 3 and 4.

Figure A.11: Global Spillovers of China's Ban—US Imports of Cryptomining Machines

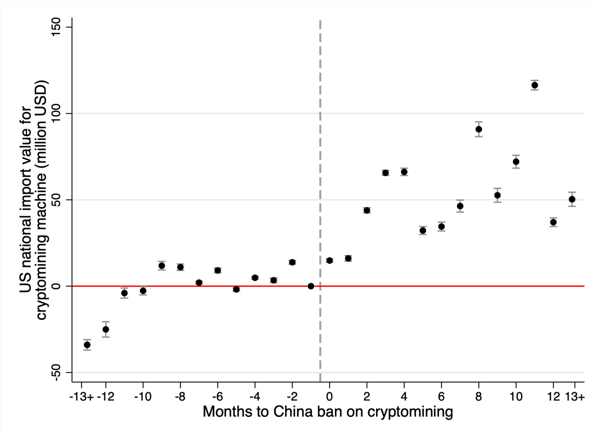

(**a**) DiD: Import value from China only

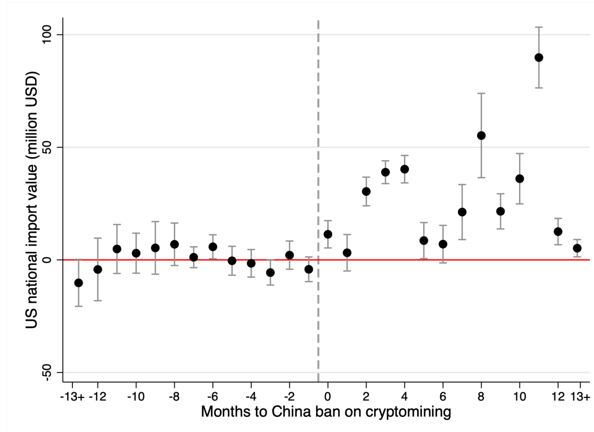

(**b**) SDiD: Import value from China only

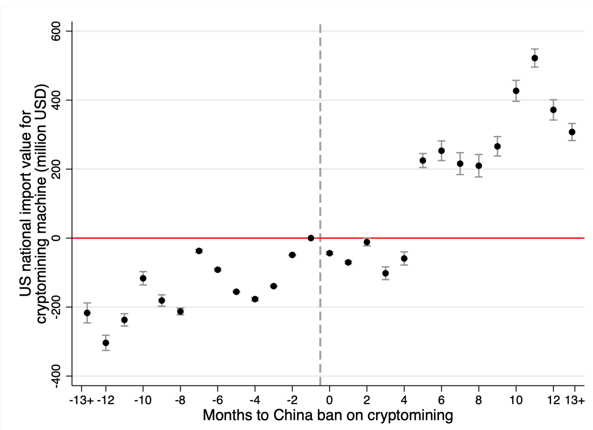

(**c**) DiD: Import value from all countries

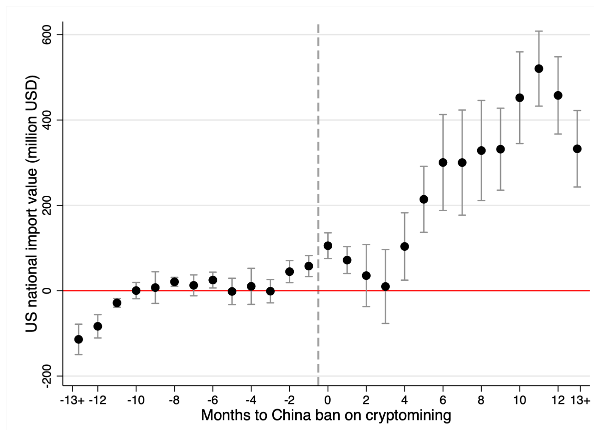

(**d**) SDiD: Import value from all countries

Notes: These figures show dynamic DiD coefficients from estimating the dynamic DiD version of equation (4). We present the set of β_k, coefficients on the $MiningEquipment_j$ dummy k months from China's ban. The dots denote point estimates and spikes 95% confidence intervals. The sample includes cryptomining machines (HS10 code 8543709960) and all other 45 HS10 products in NAICS industry 335999. The dependent variable is US imports of product j in month t from China only in panels (a)-(b) and from all origin countries in panels (c)-(d). Table A.6 reports regression estimates. Results are discussed in section 5.1.2.

Figure A.12: Global Spillovers of China's Mining Ban—Impacts on US Electricity Consumption

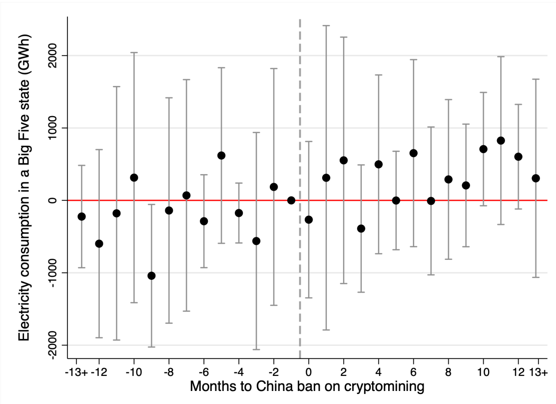

(**a**) DiD: Electricity consumption, All sectors

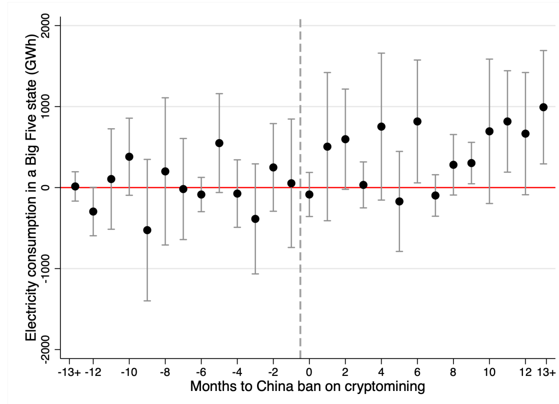

(**b**) SDiD: Electricity consumption, All sectors

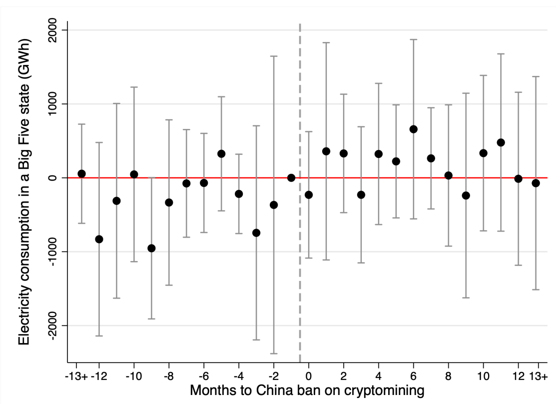

(**c**) DiD: Electricity consumption, Commercial/Industrial

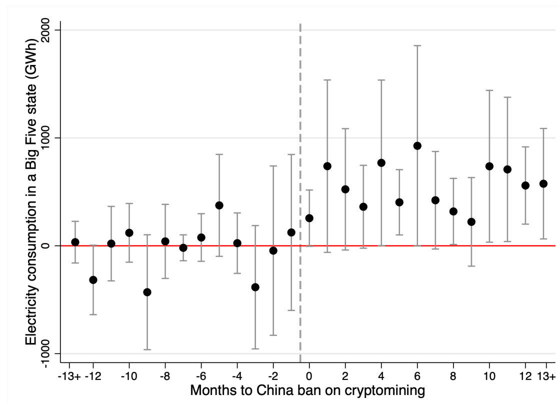

(**d**) SDiD: Electricity consumption, Commercial/Industrial

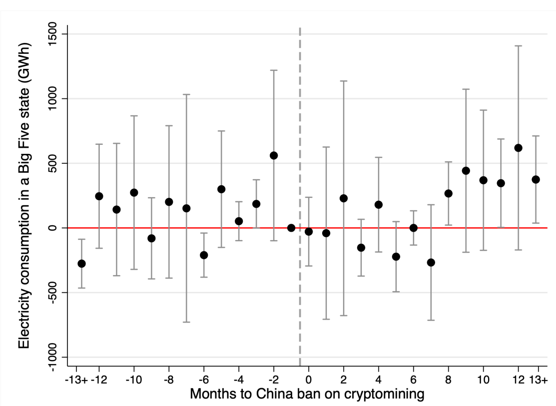

(**e**) DiD: Electricity consumption, Residential

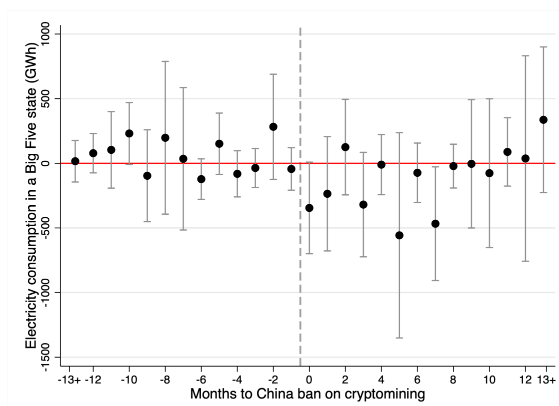

(**f**) SDiD: Electricity consumption, Residential

Notes: These figures show coefficients from estimating the dynamic DiD version of equation (6). We plot the set of β_k, coefficients on the $MiningState_i$ dummy k months from China's ban. The dots denote point estimates and spikes 95% confidence intervals. The dependent variable is total electricity consumption in panels (a)-(b), commercial and industrial consumption in panels (c)-(d), and residential consumption in panels (e)-(f). Table 5 reports regression estimates. Results are discussed in section 5.2.1.

Figure A.13: Relationship between the Age and Energy Efficiency of US Fossil-Fuel Power Plants

(**a**) Heat rate against plant age

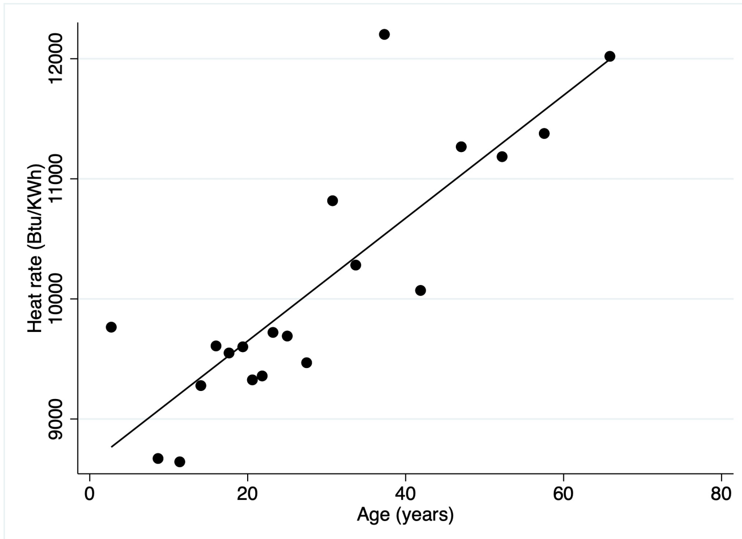

(**b**) Carbon intensity against plant age

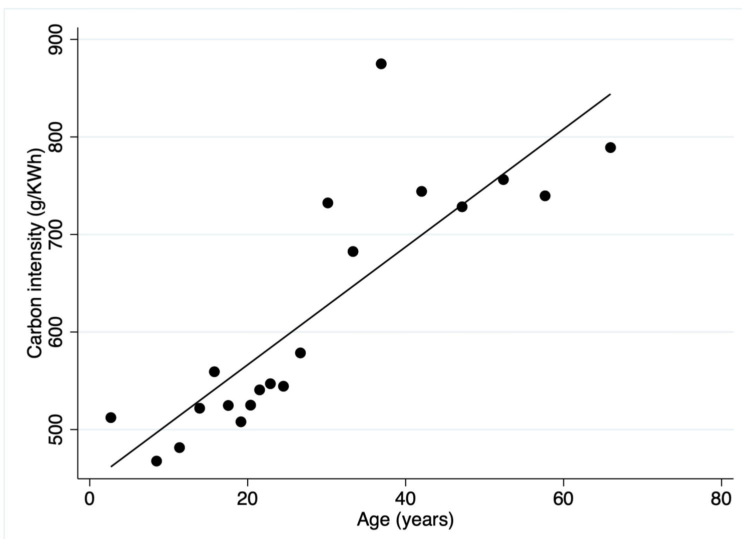

Notes: This figure shows how the heat rate (Btu/kWh, top panel) and the CO_2 emissions rate (grams/kWh, bottom panel) vary with the age of US fossil-fuel power plants (in years). The dots are means within each age bin after partialling out state, (calendar) year, and month-of-year fixed effects (the data are at the plant-month level). The plots show lines of best fit. Data sourced from the Clean Air Markets Program. Results are discussed in section 5.2.3.

Figure A.14: Impact of Ethereum's Transition on Electricity Consumption by US Balancing Authority Region

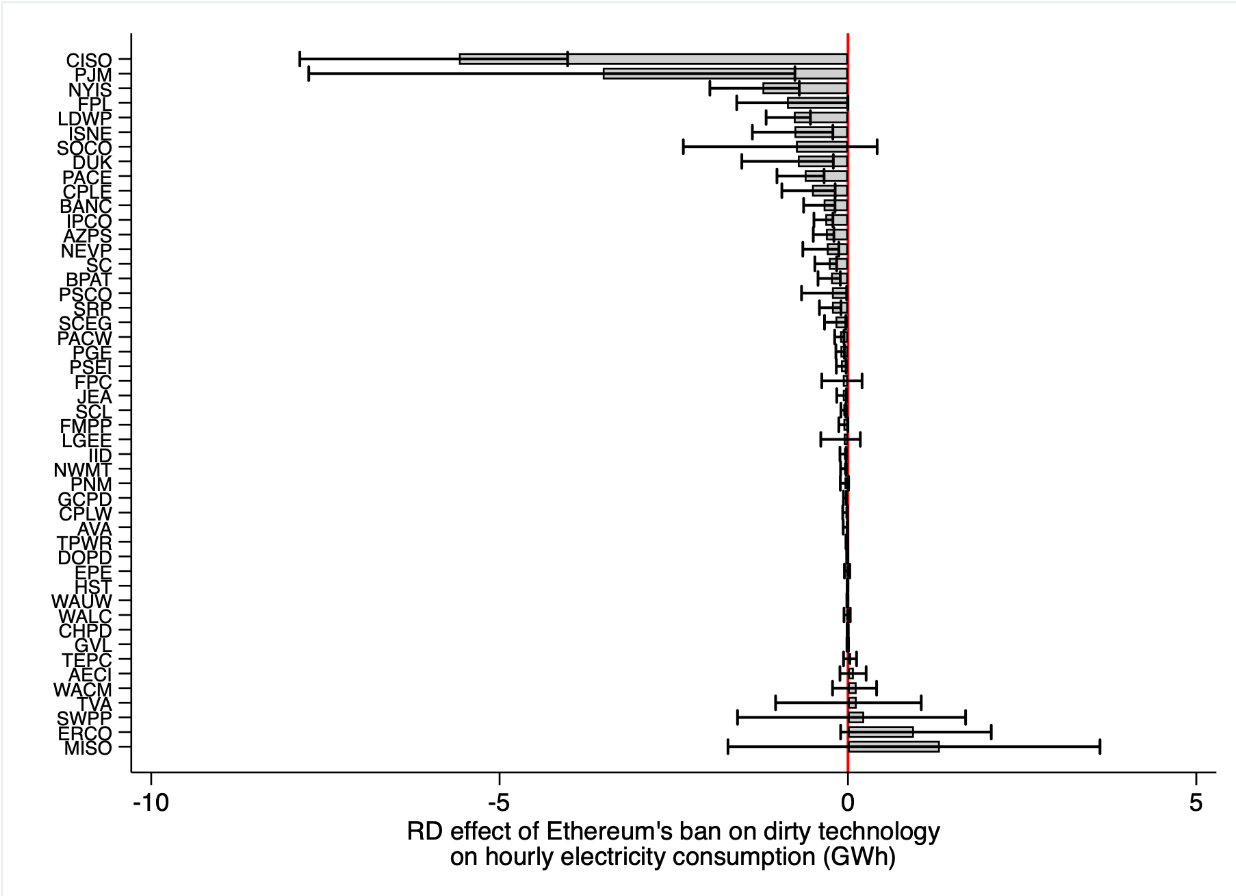

Notes: This figure plots estimates from our baseline RDiT specification (section 6.1). The dependent variable is hourly electricity consumption at the balancing authority level (GWh). We estimate the RDiT model separately for each balancing authority using the same baseline specification and employ a 30-day bandwidth. We abbreviate the names of balancing authorities when labeling the vertical axis. The gray bars report point estimates and the whiskers show 95% confidence intervals bootstrapped using 500 repetitions. Table 7 reports average estimates. Results are discussed in section 6.2.

Figure A.15: Impact of Ethereum's Transition on Electricity Consumption by US State

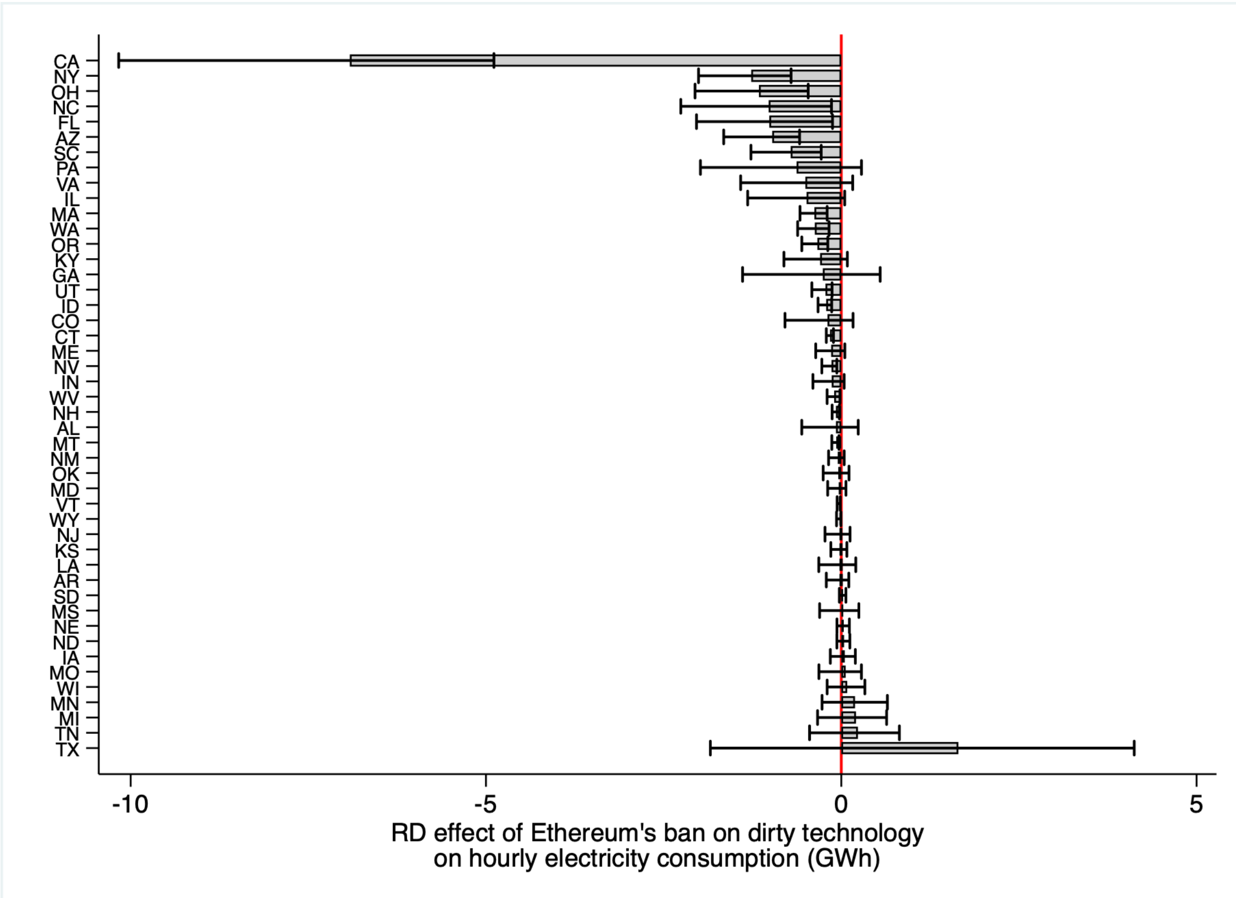

Notes: This figure plots estimates from our baseline RDiT specification (section 6.1). The dependent variable is hourly electricity consumption at the state level (GWh). We estimate the RDiT model separately for each state using the same baseline specification and employ a 30-day bandwidth. The gray bars report point estimates and the whiskers show 95% confidence intervals bootstrapped using 500 repetitions. Table 7 reports average estimates. Results are discussed in section 6.2.

Figure A.16: Impact of Ethereum's Transition on Mining Activity of Other Cryptocurrencies

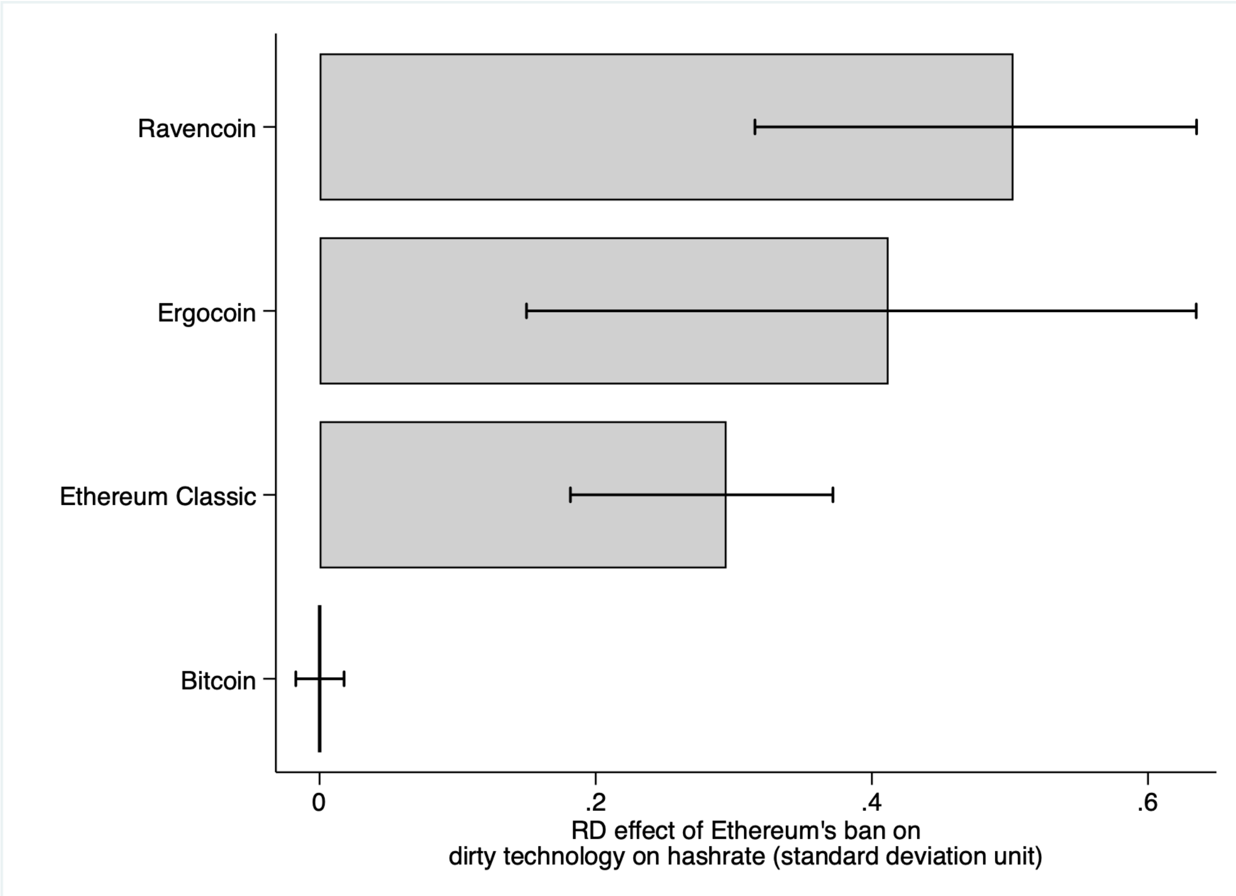

Notes: The figure plots estimates from our baseline RDiT specification (section 6.1). The dependent variable is the standardized daily global hashrate for each cryptocurrency. Separately by cryptocurrency, in a first stage we regress the standardized hashrate on its daily closing price, weather controls (5°C wide temperature bins, precipitation and its square, dew point depression, and wind speed), and time fixed effects (month-of-sample, year-by-day-of-week fixed effects, and federal holiday) using data between 1 January 2021 and 31 December 2023. In the second stage, we estimate the RD regression. The dependent variable are first-stage residuals, and the running variable is days before/after Ethereum's transition to PoS on 15 September 2022. We use a 30-day bandwidth similar to column 1 of table 7. The gray bars report point estimates and the whiskers show 95% confidence intervals bootstrapped using 500 repetitions. Results are discussed in section 6.3. RD graphs are presented in figure 4.